Overview of Interfacial Area Transport in Multiphase Flow Systems

Xiaodong Sun
Nuclear Engineering Program
Department of Mechanical Engineering
The Ohio State University

October 17, 2007

Outline of Presentation

- Research Background
- Experiments
- Modeling
  - One-group Interfacial Area Transport Equation
  - Two-group Interfacial Area Transport Equation
- Implementation of One-group IATE
- Summary and Conclusions

Research Background

- Two-fluid Model and Interfacial Area Concentration
- Interfacial Area Transport Equations

Challenge: Interfacial Structure Characterization in Gas-liquid Two-phase Flows


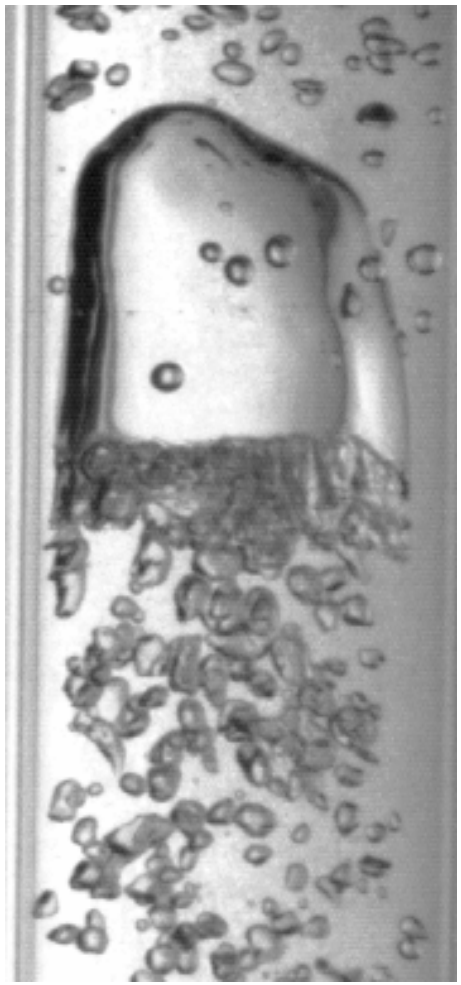
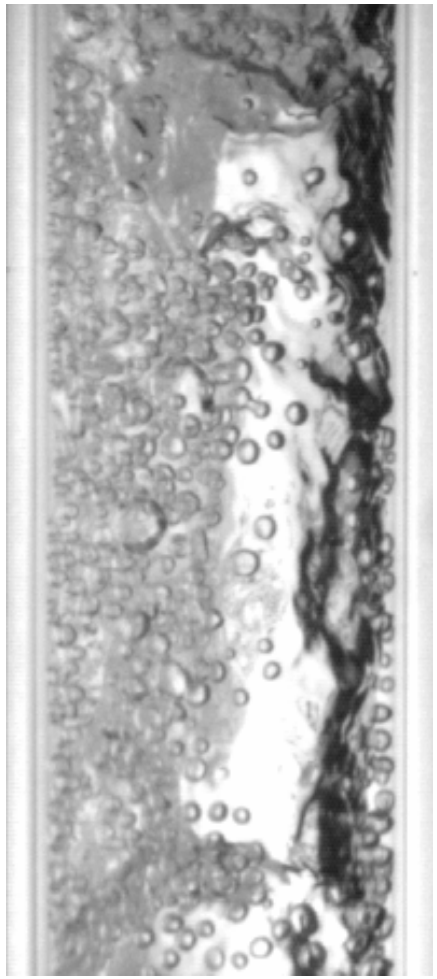

Flow Regimes/Patterns in Upward Flow
Air-water, 25.4 mm ID Pipe

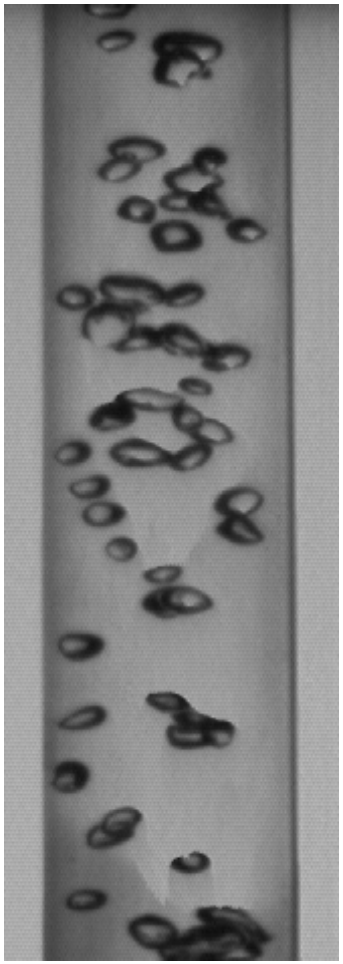

Bubbly

Cap-bubbly

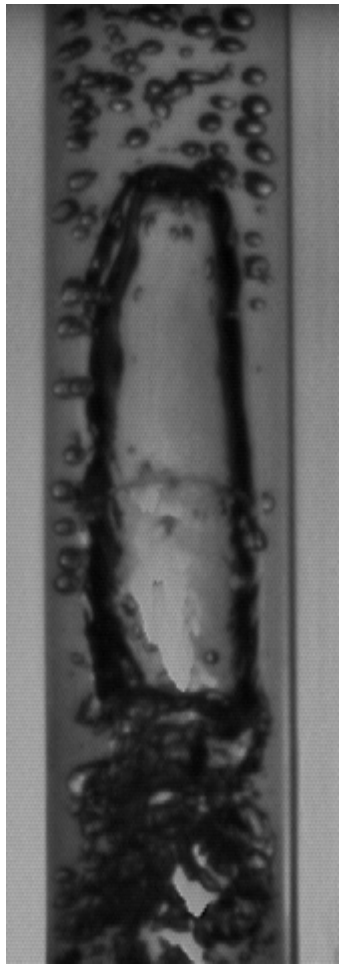

Slug

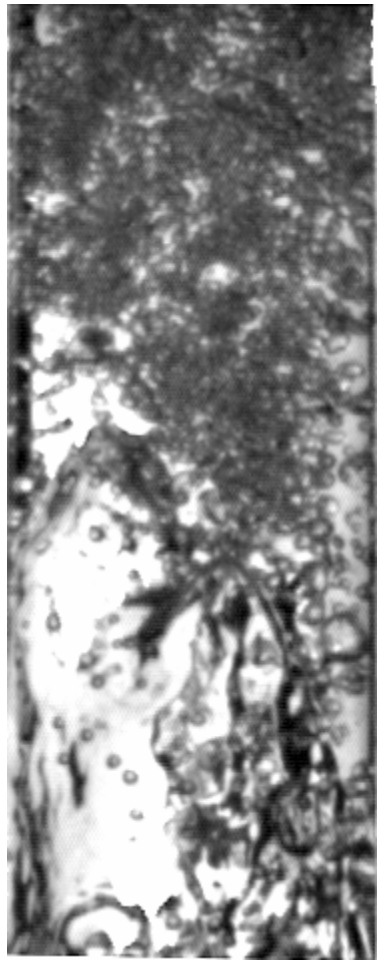

Churn-turbulent

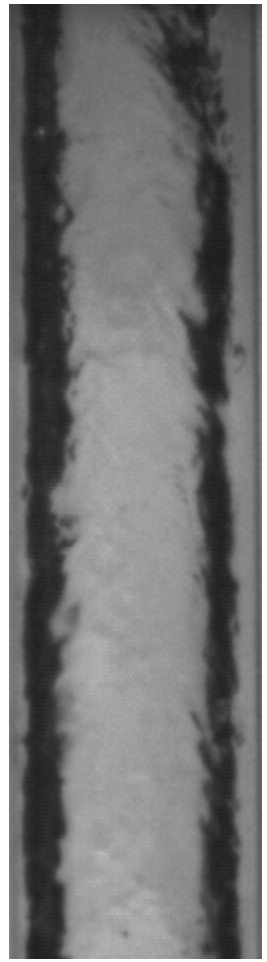

Annular

Flow

Gas-liquid Two-phase Flow Modeling

- Main Difficulties in Two-phase Flow Modeling
  - Existence of Interfaces between Phases
  - Discontinuities Associated with the Interfaces
- Two-phase Flow Modeling
  - Eulerian Time (Statistical) Averaging
  - Represented by Macroscopic Field Equations and Constitutive Relations using Continuum Formulation
- Two-fluid Model (Vernier and Delhaye, '68; Ishii, '75; Drew and Lahey, '79)
  - Considers Each Phase Separately
  - Macroscopic Fields of one Phase are coupled to the Other Phase
  - Interfacial Transfer Terms in the Conservation Equations

Two-fluid Model Conservation Equations

- Continuity Equation

$$\frac{\partial \alpha_k \rho_k}{\partial t} + \nabla \cdot (\alpha_k \rho_k \vec{v}_k) = \Gamma_k$$

- Momentum Equation

$$\frac{\partial \alpha_k \rho_k \vec{v}_k}{\partial t} + \nabla \cdot (\alpha_k \rho_k \vec{v}_k \vec{v}_k) = -\nabla (\alpha_k p_k) + \nabla \cdot \alpha_k (\bar{\bar{\tau}}_k + \bar{\bar{\tau}}_k^t) + \alpha_k \rho_k \vec{g}$$

$$+ p_{ki} \nabla \alpha_k + \vec{v}_{ki} \Gamma_k + \vec{M}_{ik} - \nabla \alpha_k \cdot \bar{\bar{\tau}}_i$$

- Energy Equation

$$\frac{\partial \alpha_k \rho_k H_k}{\partial t} + \nabla \cdot (\alpha_k \rho_k H_k \vec{v}_k) = -\nabla \cdot \left[\alpha_k (\vec{q}_k + \vec{q}_k^t)\right] + \alpha_k \frac{D_k p_k}{Dt}$$

$$+ H_{ki} \Gamma_k + a_i q''_{ki} + \phi_k$$

Interfacial Area Concentration: a_i

Interfacial Area Concentration

- (Interfacial Transfer): ~ (Interfacial Area Concentration) × (Driving Potential)
- Interfacial Area Concentration, a_i

$$a_i = \frac{\text{Interfacial Area}}{\text{Mixture Volume}}$$

  - Characterizes the Geometric "Capacity" for Interfacial Transfer

- Conventional Approach: Flow Regime-dependent Correlations/Models
  - Flow Regime Identified by Flow Regime Map or Regime Transition Criteria (Bubbly, Slug, Churn, …)
  - Some Shortcomings

Flow Regime Map for Vertical Upflow

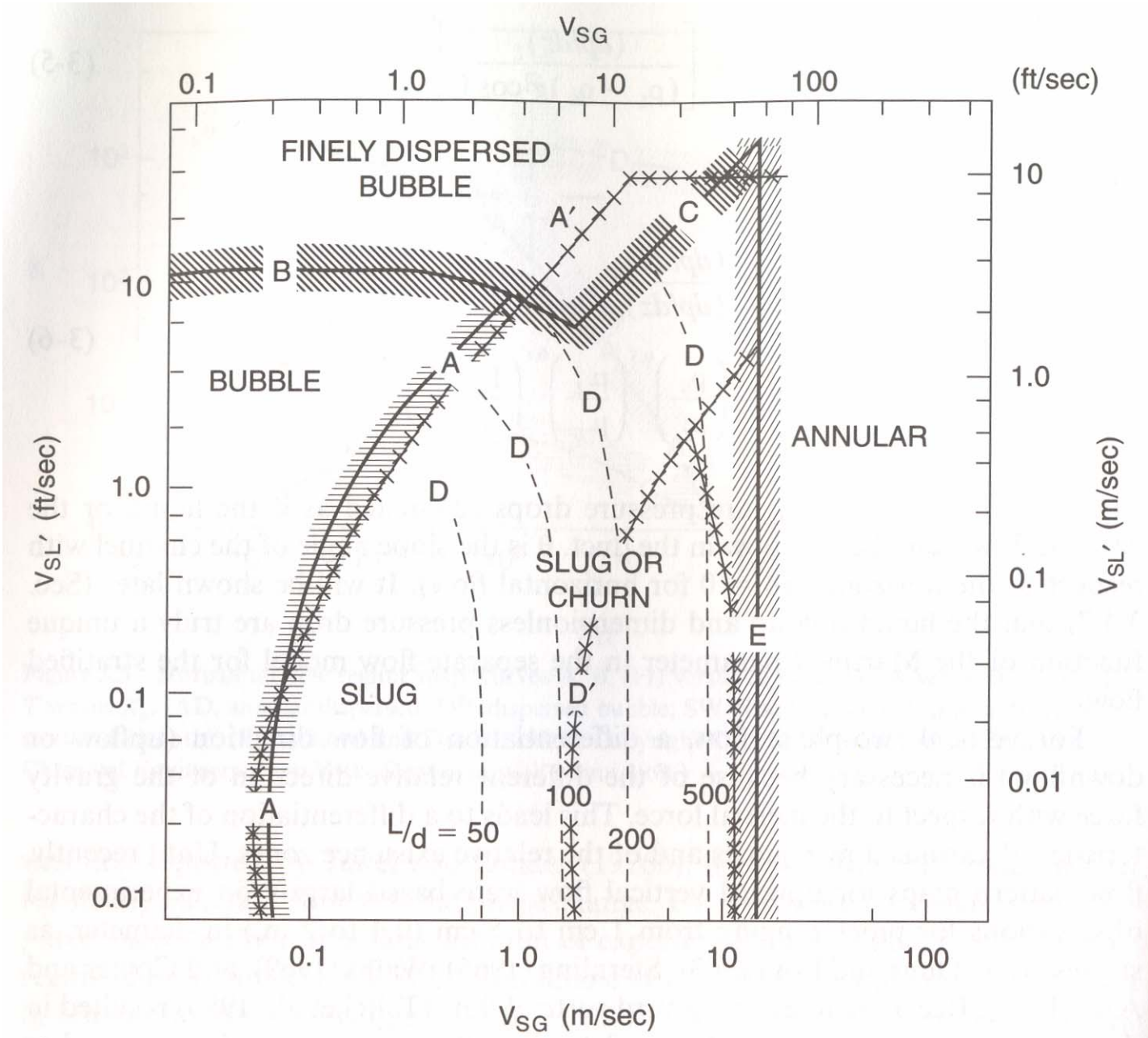

Taitel and Dukler
Mishima and Ishii

Shortcomings of Flow Regime-based Approach

- Inconsistency with the Two-fluid Model Formulation
  - Phase Interaction: Dynamic (through Field Equations)
  - Interfacial Geometry Modeling: Static (Flow Regimes)

- Flow Regime Map: Developed for Fully-developed Flow
  - Difficulty in Modeling Effects of Entrance, Flow Development, and Phase Change

- Introduction of Bifurcation into Codes
  - Through Flow Regime Transition Criteria (Switches)
  - May lead to Numerical Oscillations

Interfacial Area Transport Equation

- Dynamic Approach for Interfacial Structure Modeling, Consistent with the Two-fluid Model (Ishii, '75)
- Predict Evolution of Interfacial Structures Dynamically
- Foundation of Interfacial Area Transport Equation (IATE) (Ishii & Kojasoy, '95)

$$\frac{\partial a_i}{\partial t} + \nabla \cdot \left(a_i \vec{v}_i \right) = \sum_j \phi_j + \phi_{\mathrm{ph}}$$

Source/sink terms need to be modeled

About Bubbles

- Bubbles change their size and shape as they grow
- Spherical Bubbles → Distorted Bubbles → Cap Bubbles → Slug Bubbles → Churn-turbulent Bubbles

Spherical bubble limit: $D_{ds} = 4\sqrt{\frac{2\sigma}{g\Delta\rho}}N_{\mu_f}^{1/3}; \quad N_{\mu_f} = \frac{\mu_f}{\left(\rho_f \sigma\sqrt{\frac{\sigma}{g\Delta\rho}}\right)^{1/2}}$

Distorted bubble limit: $D_{d\,max} = 4\sqrt{\frac{\sigma}{g\Delta\rho}}$

Cap bubble limit: $D_{c\,max} = 40\sqrt{\frac{\sigma}{g\Delta\rho}}$

Large Bubble Breakup due to Instability
(500 Frames/s)

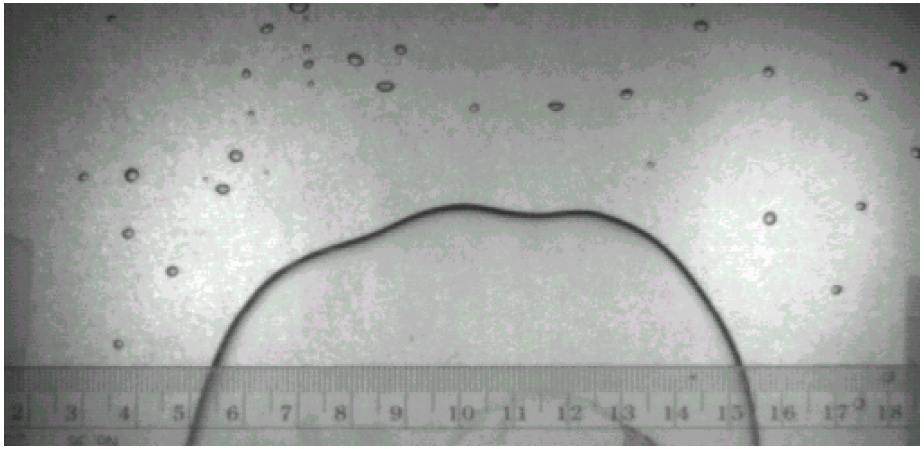

t=0

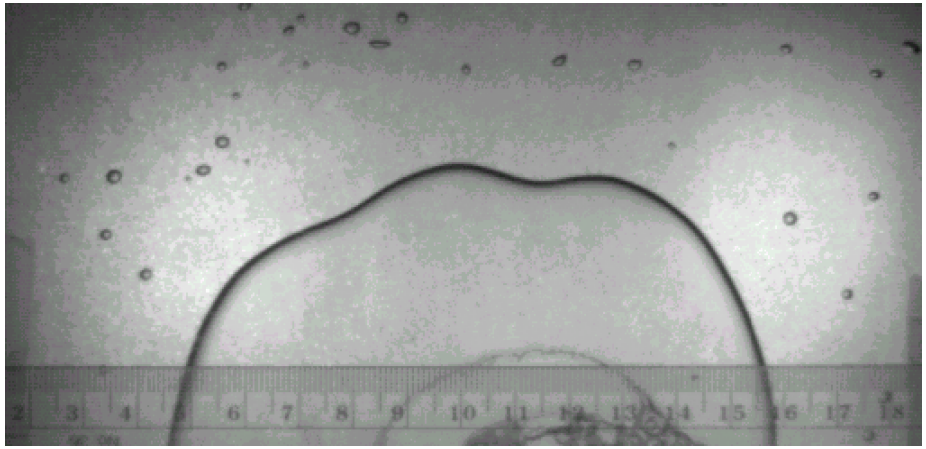

t=20 ms

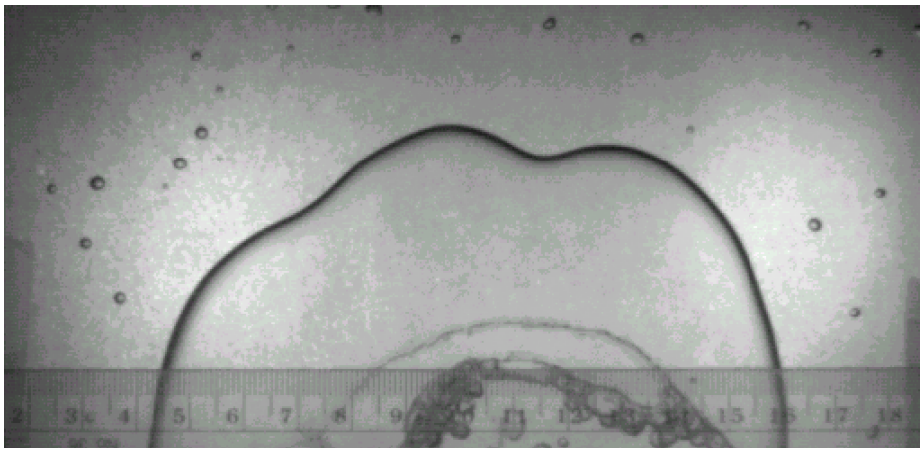

t=40 ms

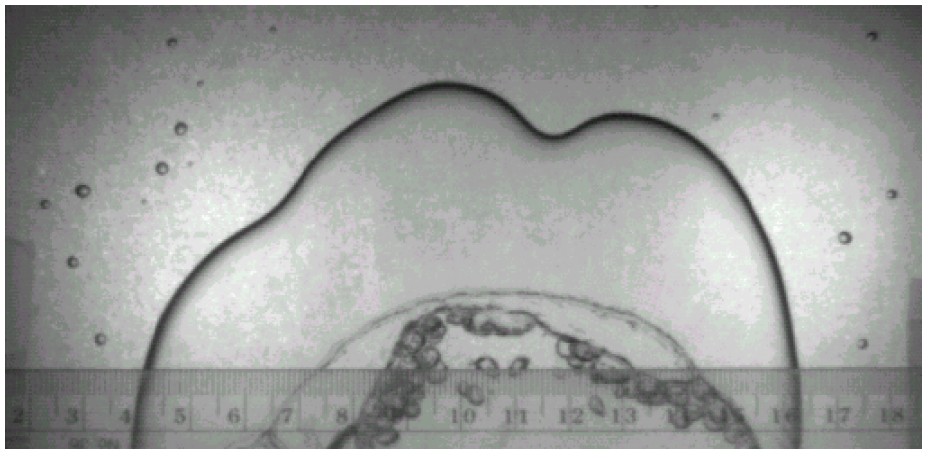

t=60 ms

Large Bubble Breakup due to Instability (Cont'd)

(500 Frames/s)

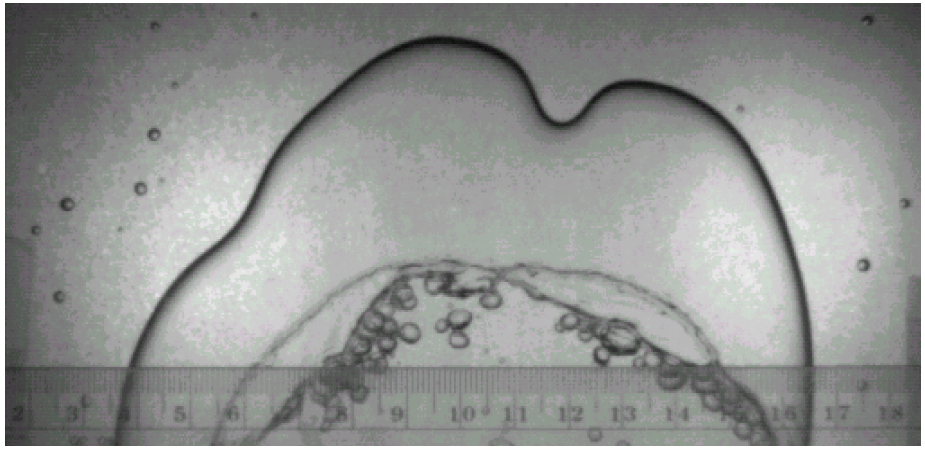

t=80 ms

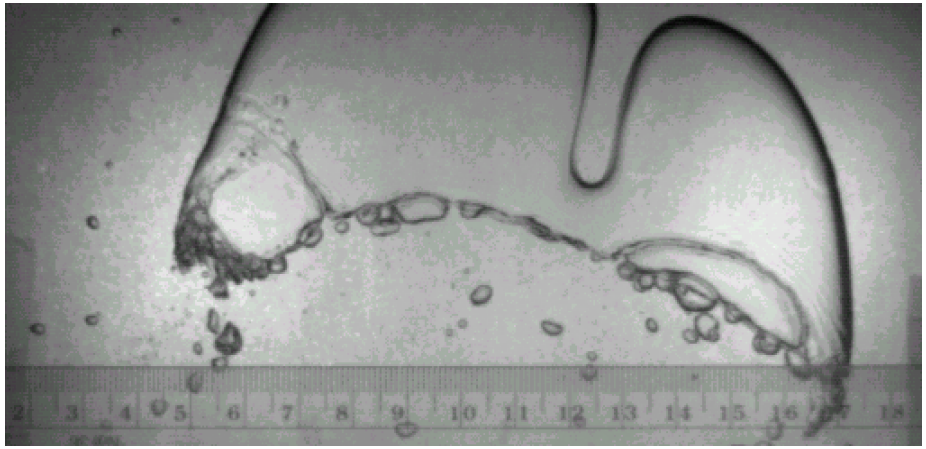

t=140 ms

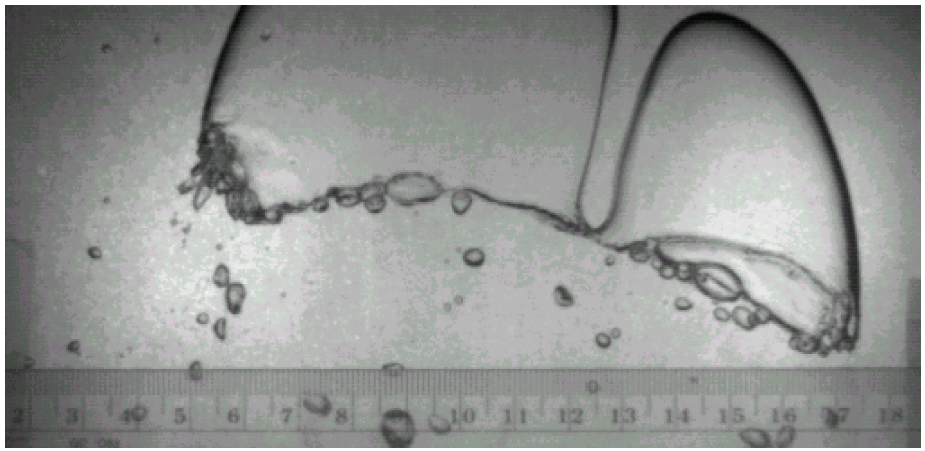

t=156 ms

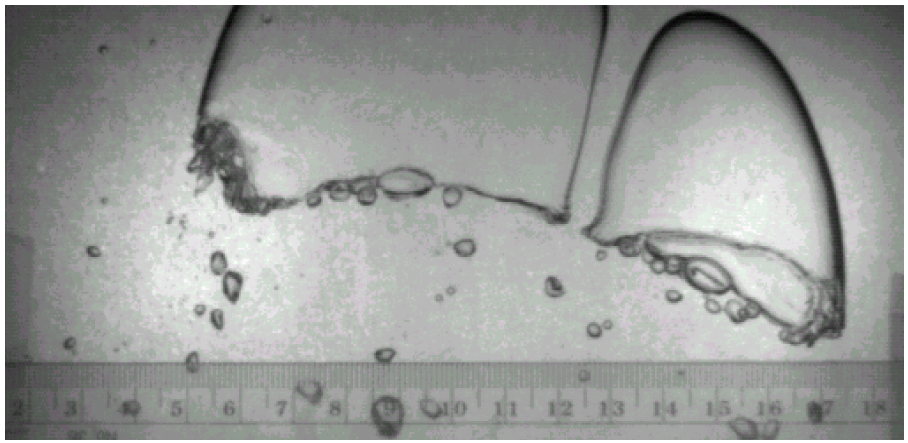

t=158 ms

Research Objectives

- To Develop Interfacial Area Transport Equation to Dynamically Predict the Change of Interfacial Area Concentration
- To Model Bubble Interaction Mechanisms
- To Build a Reliable Database in a Wide Range of Flow Conditions
- To Evaluate the Transport Equation based on the Acquired Experimental Database
- To Implement the IATE to a CFD Code and/or a Safety Analysis Code

Experiments

- Multi-sensor Conductivity Probes
- Local Measurement Results

Measurement Techniques of Multi-sensor Conductivity Probe

- Measurement Principle: Based on Difference of Electric Conductivity between the Gas and Liquid Phases
- Measurement Principle of Local Time-averaged a_i (Ishii, '75)

$$\overline{a}_i^t = \frac{1}{\Delta T}\sum_j \left(\frac{1}{|\vec{v}_i \cdot \vec{n}_i|}\right)_j$$

- Kataoka & Ishii ('84): Measurement Formulations for Double- and Four-sensor Conductivity Probes
- Kim et al. ('98)
  - Miniaturizing four-sensor probe
  - Minimizing number of missing bubbles and deformation of bubble interface
  - Bubble categorization for different types of bubbles $D_{d,\max} = 4\sqrt{\frac{\sigma}{g\Delta\rho}}$

Schematic of Four-sensor Conductivity Probe

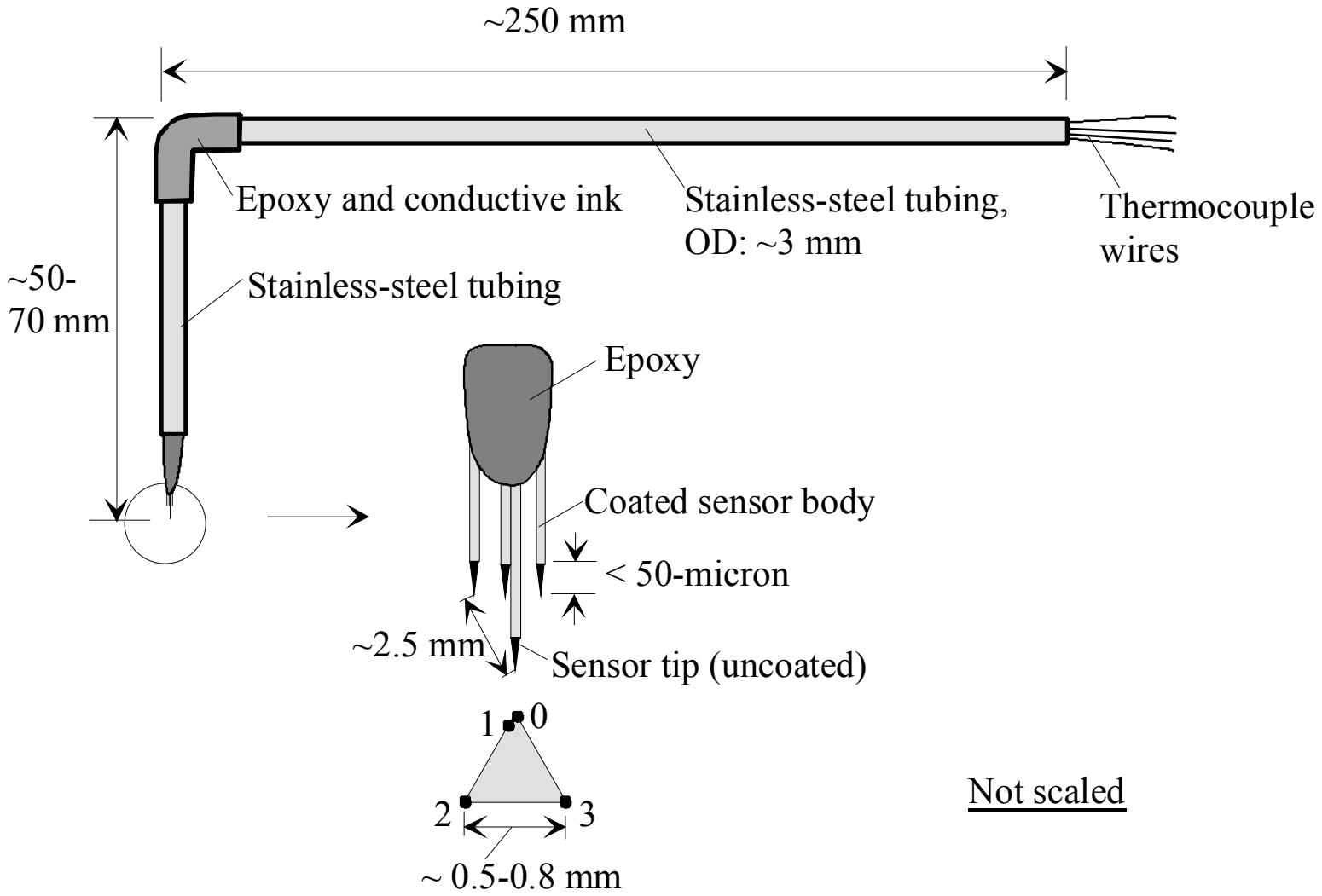

Measurement Principle of Conductivity Probe

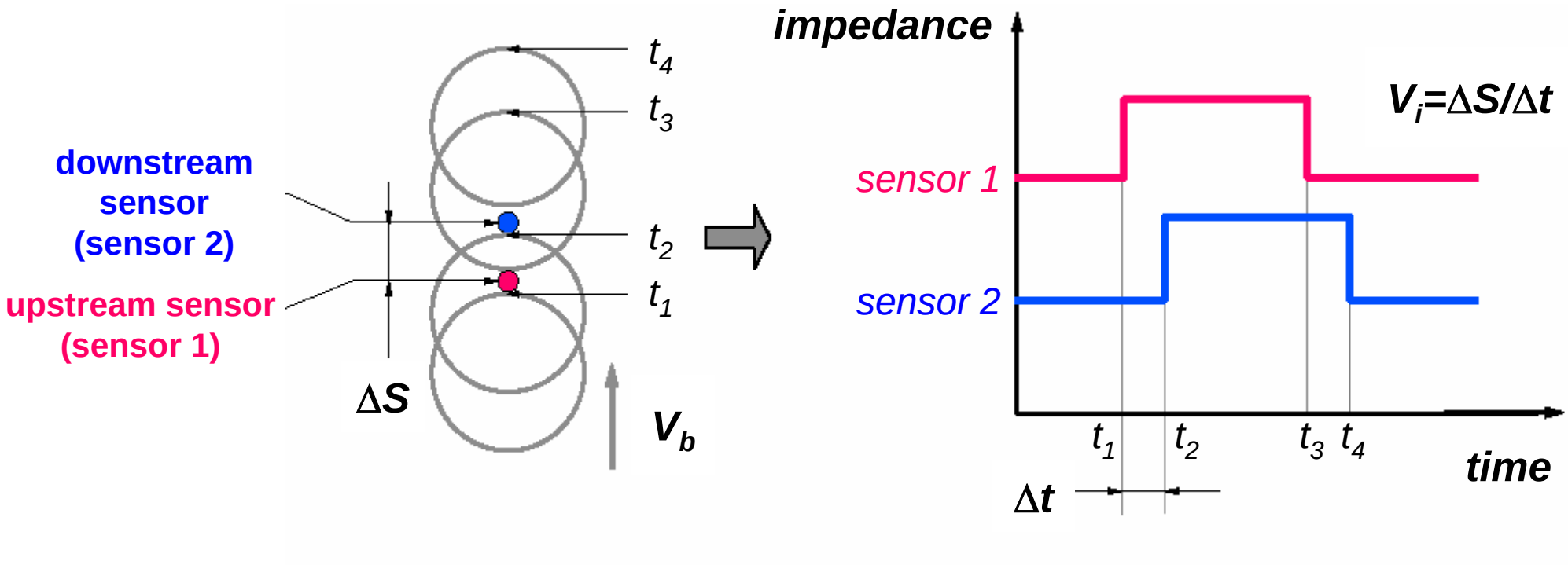

Conductivity Probe Sensor

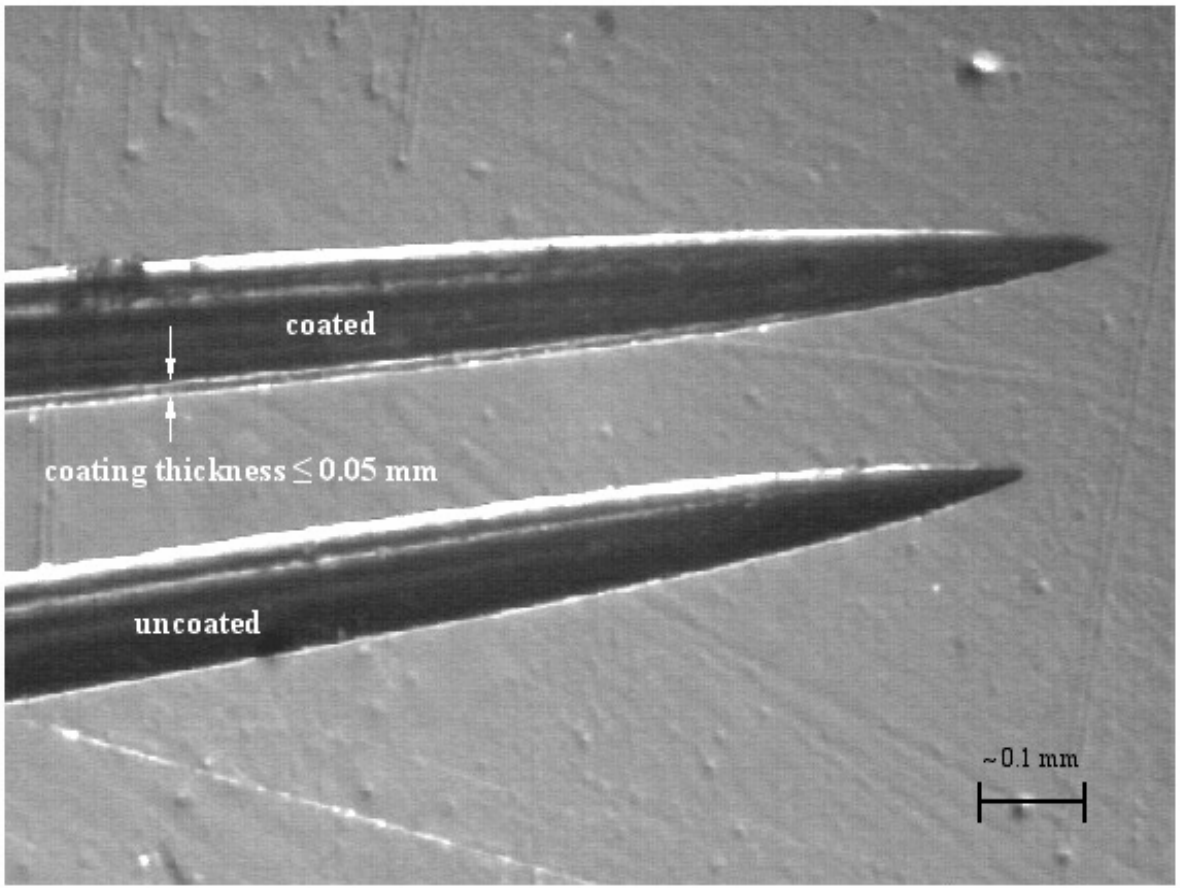

Probe Traverse Mechanism

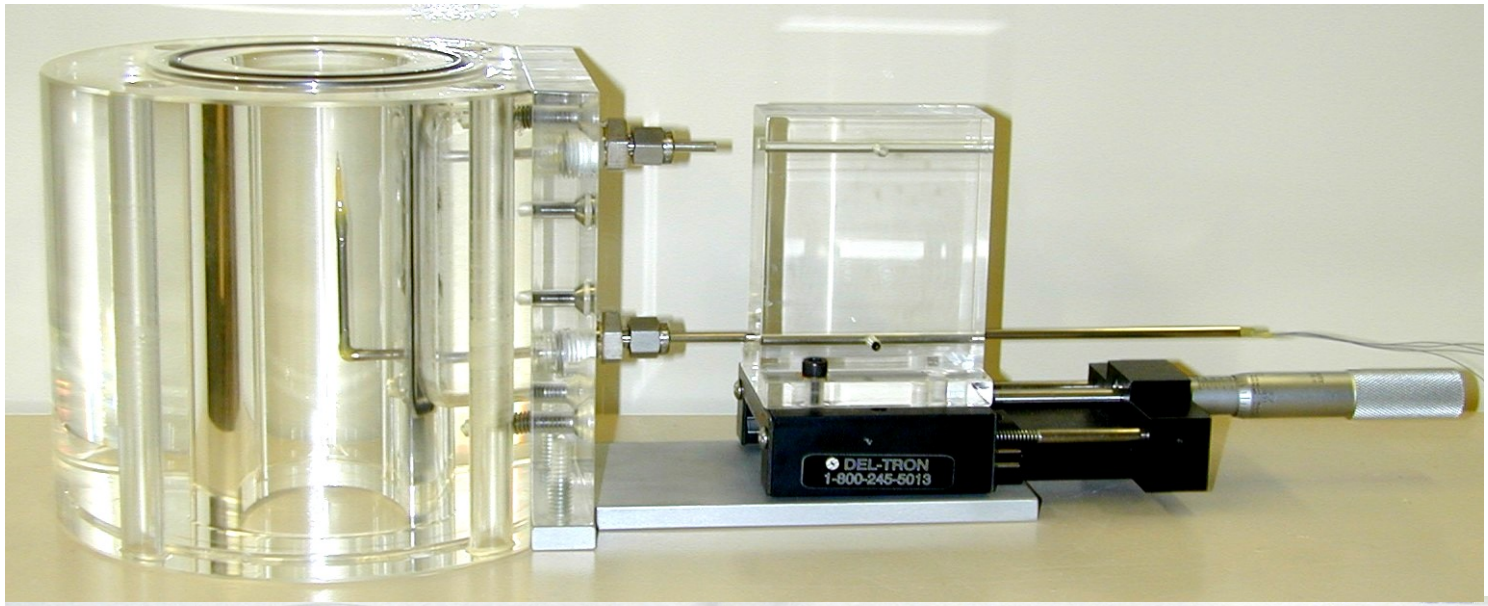

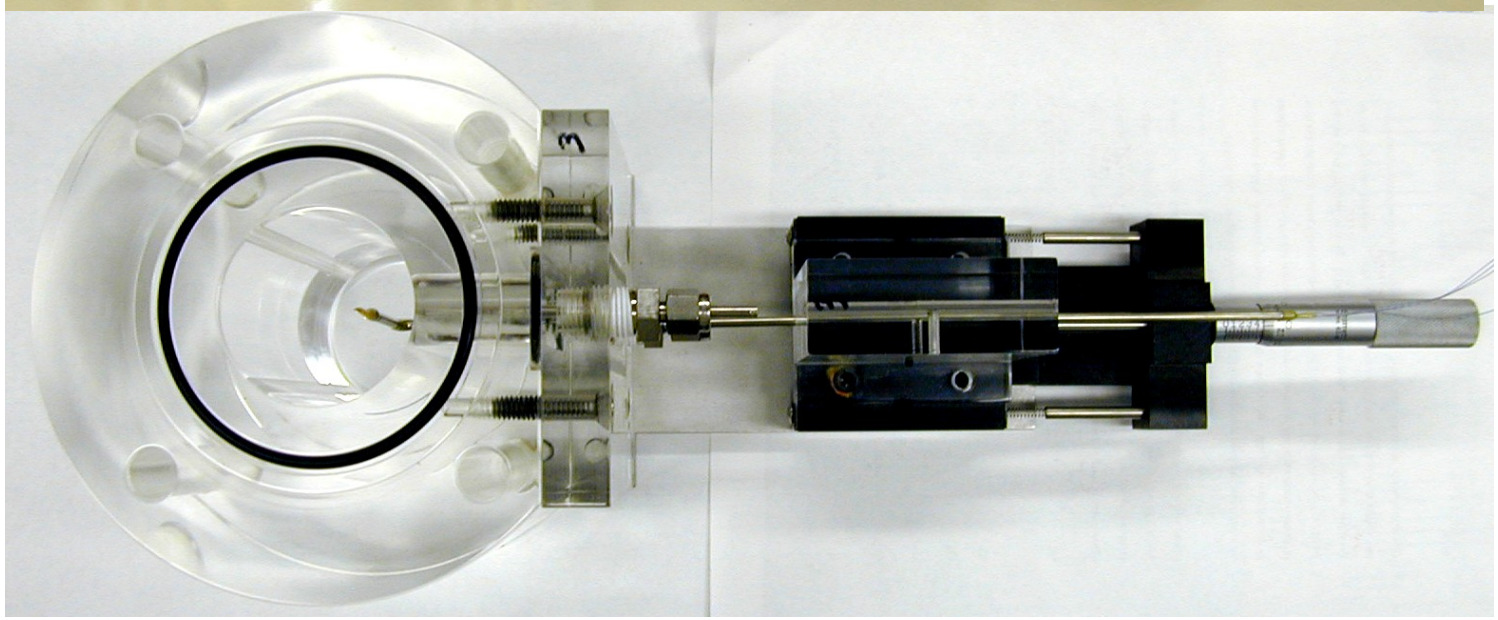

Benchmark with Gamma Densitometer

(5.08 cm ID Pipe Upward Flow)

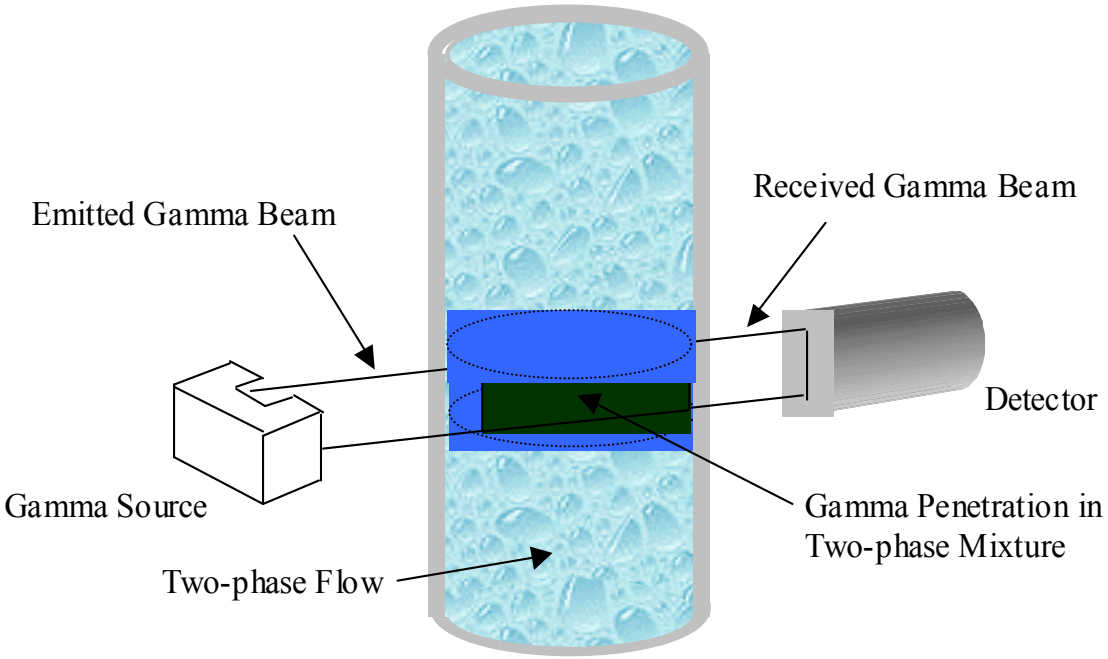

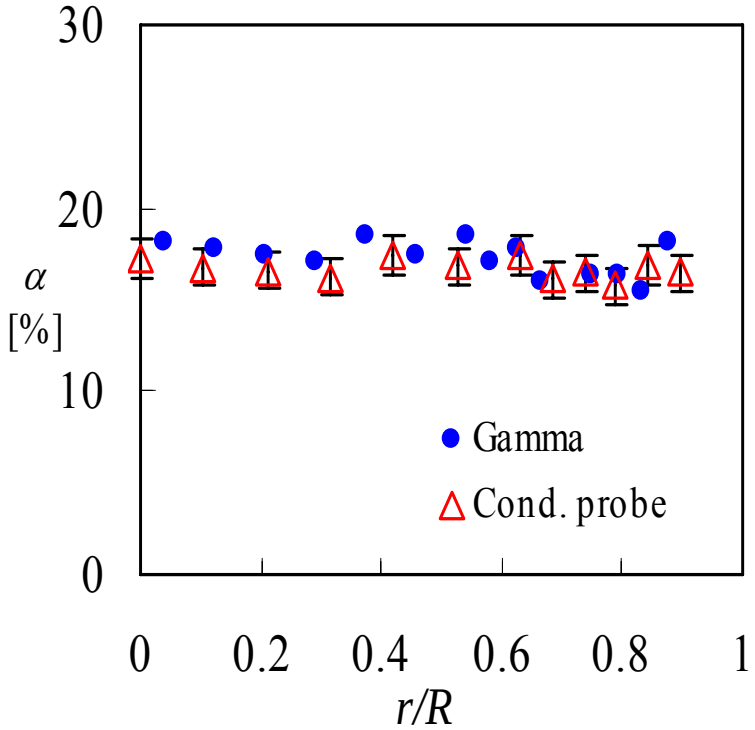

Comparison for Bubbly Flow

Error Bar: ±5%

Benchmark with Image Analysis

(5.08 cm ID Pipe Upward Flow: j_f = 0.321 and j_g = 0.179 m/s)

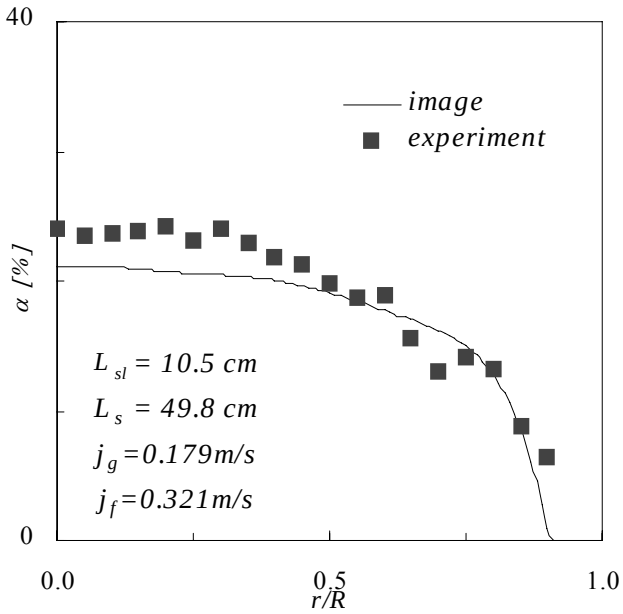

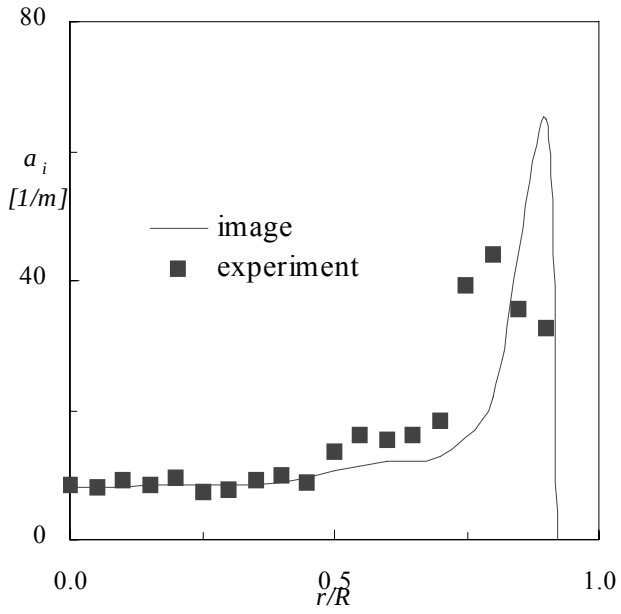

Comparison for Slug Flow

Experimental Facility

- Co-current, Vertical Air-water Two-phase Flow Loop
- Confined Rectangular Test Section
  - Cross Section: 200×10 mm^2
  - Advantage for Flow Visualization of Flow Structures: No Image Distortion Associated with Curved Surface
  - 6 Measurement Ports along Flow Direction: z/D_h: 8.0, 34.8, 61.5, 88.2, 115.0, and 141.7
- Unique Bubble Injection Units
  - Six Spargers with Porous Material (Sintered Metal): Average Pore Size 10 micron
  - To Generate Bubbles of Nearly Uniform Size at the Inlet

Schematic of Experimental Facility

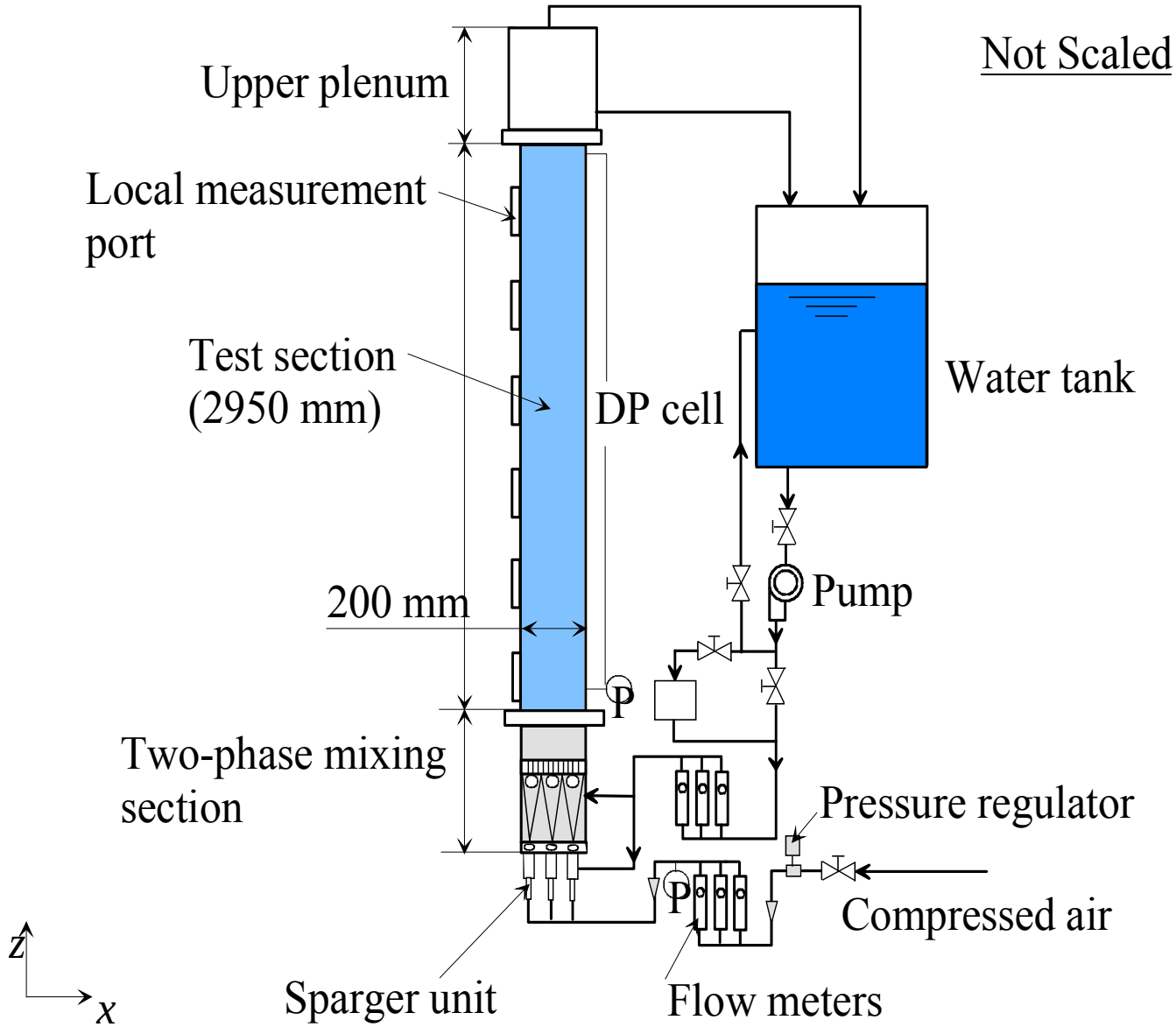

Images for Bubbly, Cap and Churn-turb. Flows

Bubbly

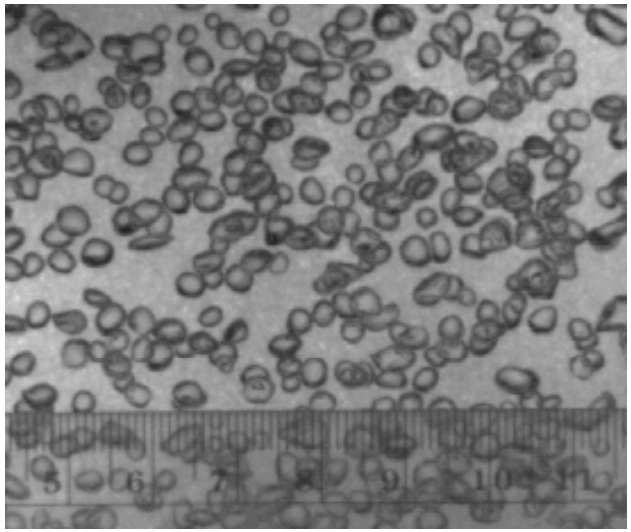

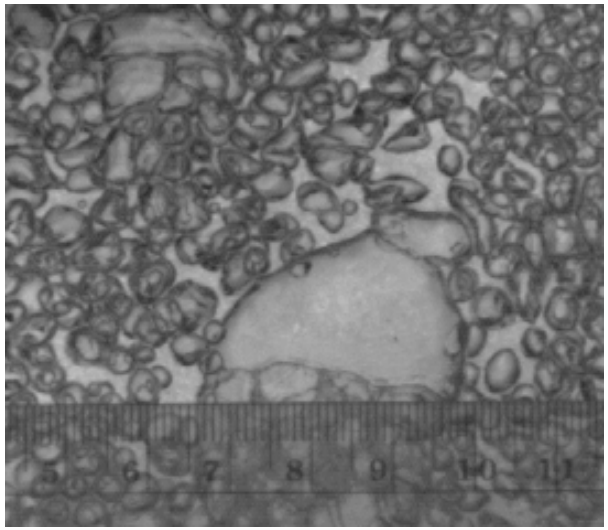

Cap-bubbly

Churn-turbulent

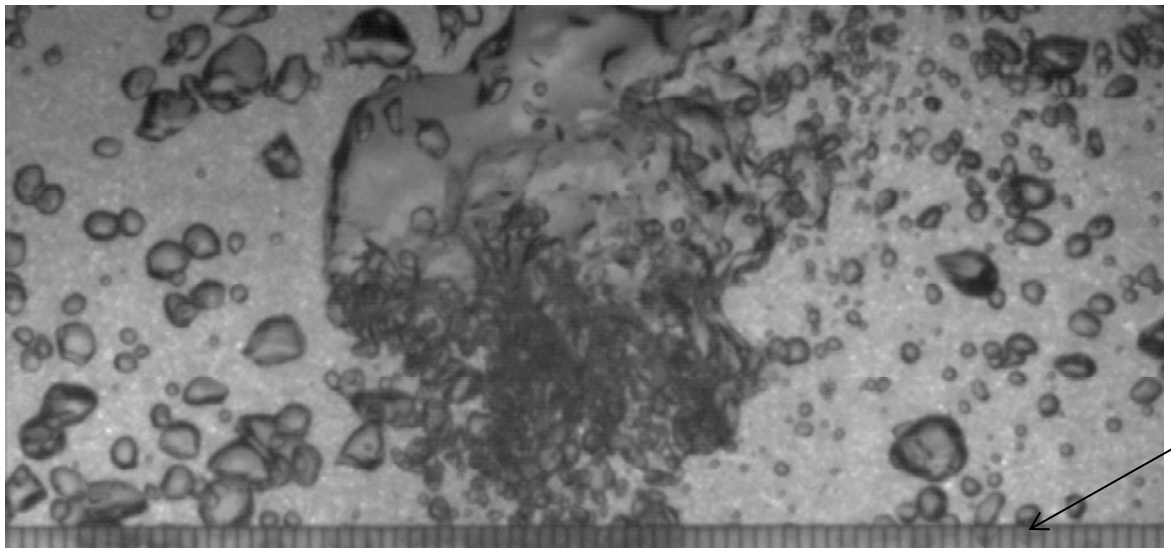

Scale: 1 mm

Experimental Flow Conditions

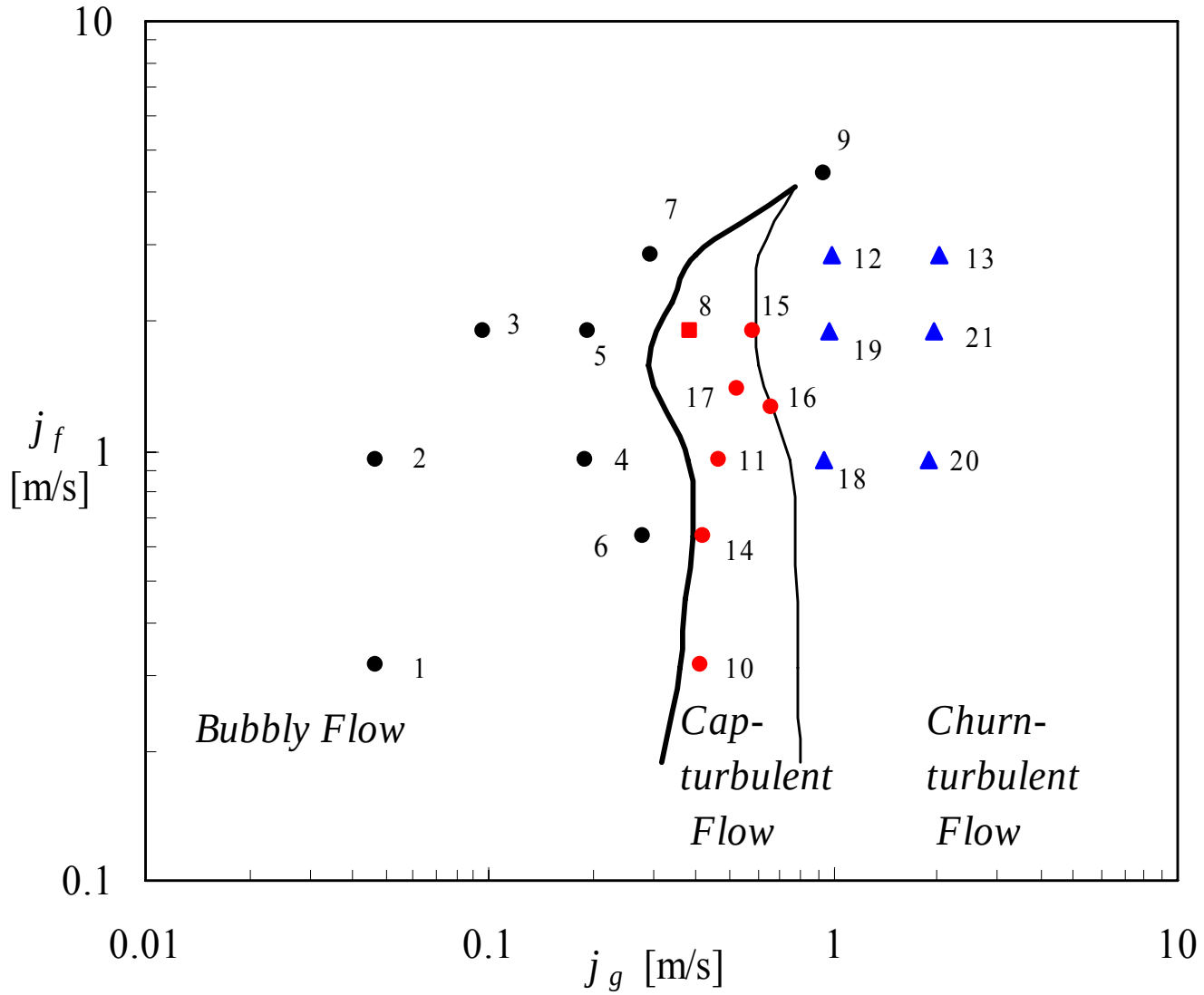

Measurement Mesh for Local Conductivity Probe

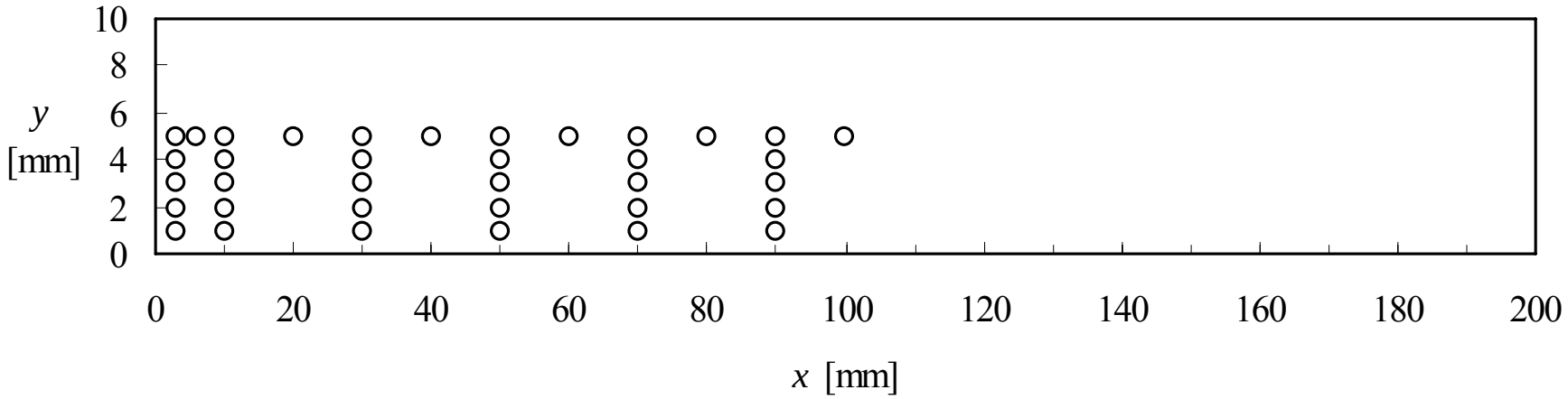

Measurement Points at Each Measurement Port

Not Scaled

Data of Run 12: Void Fraction
(j_f = 2.84 and j_{g0} = 1.0 m/s)

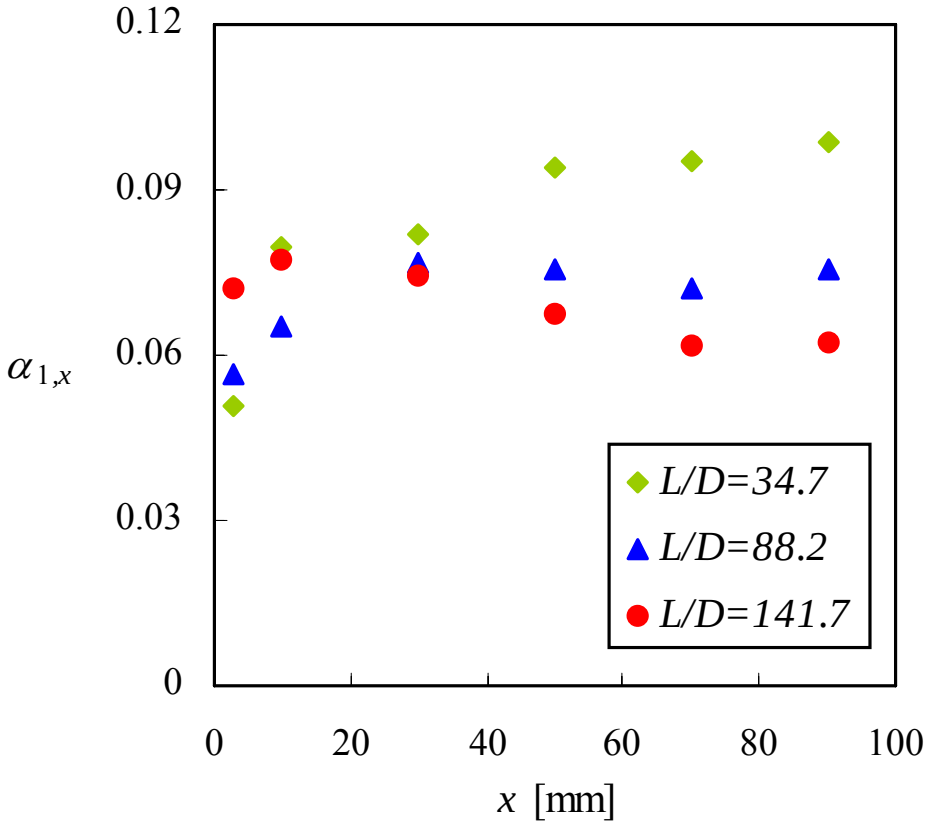

Group 1

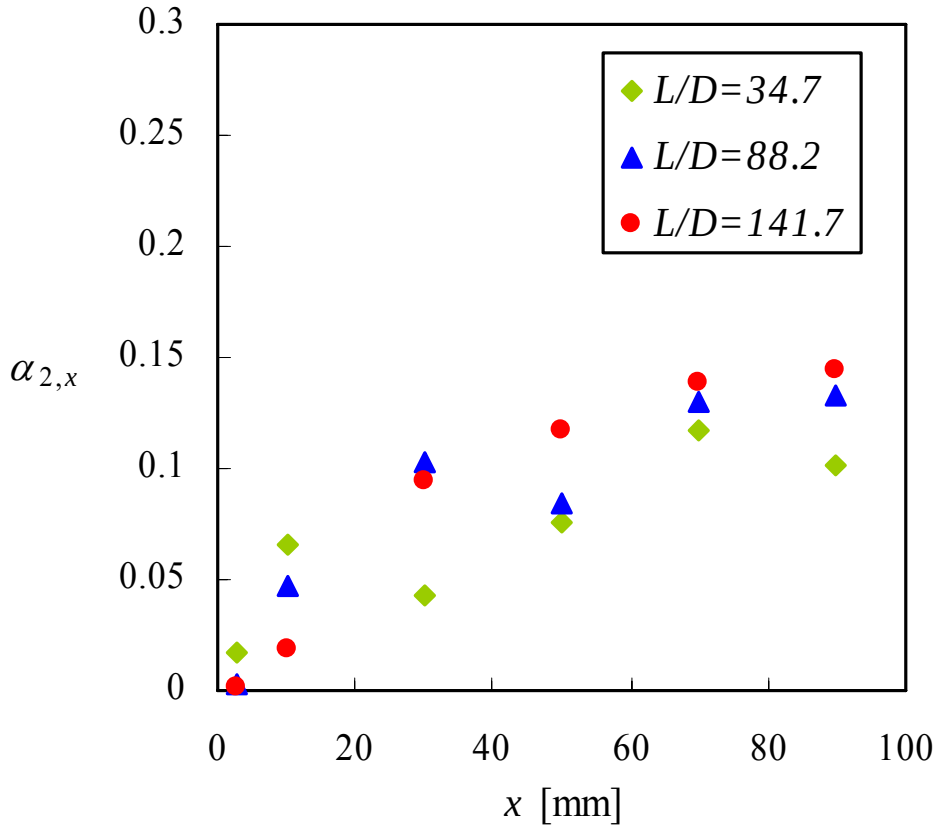

Group 2

Data of Run 12: IAC
(j_f = 2.84 and j_{g0} = 1.0 m/s)

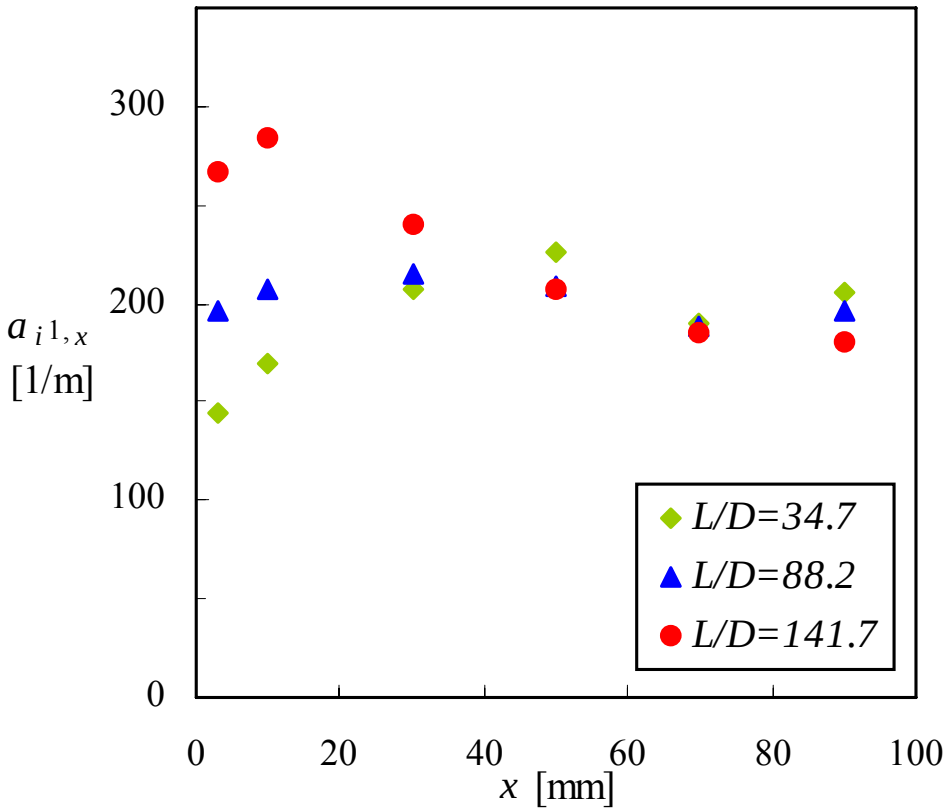

Group 1

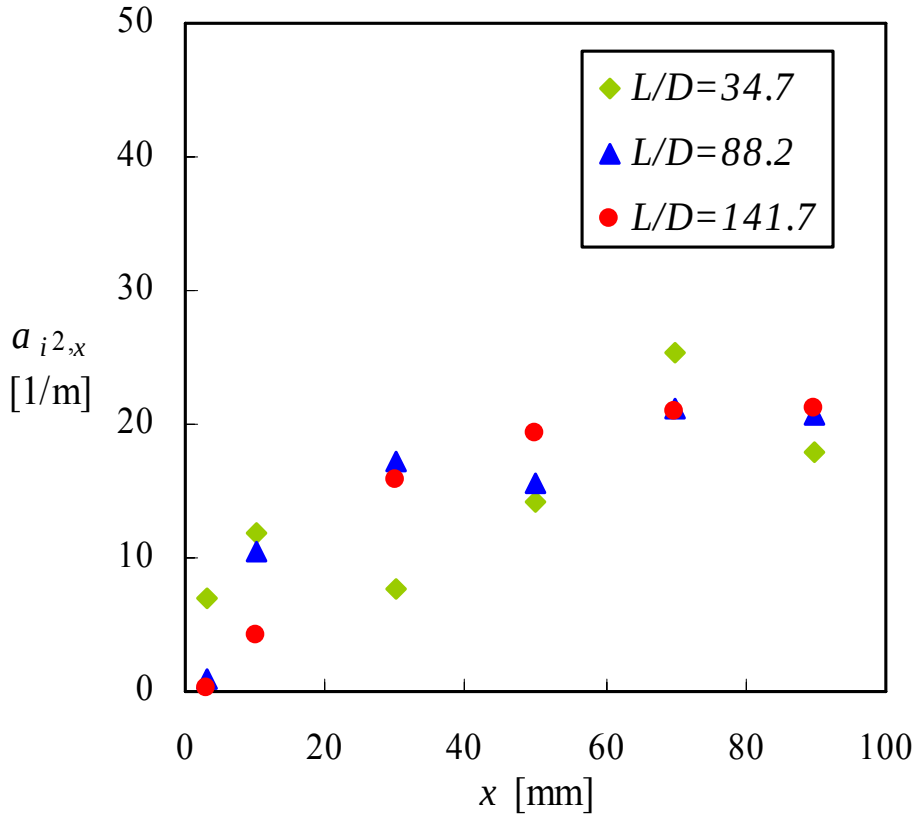

Group 2

Data of Run 12 : D_{sm}
(j_f = 2.84 and j_{g0} = 1.0 m/s)

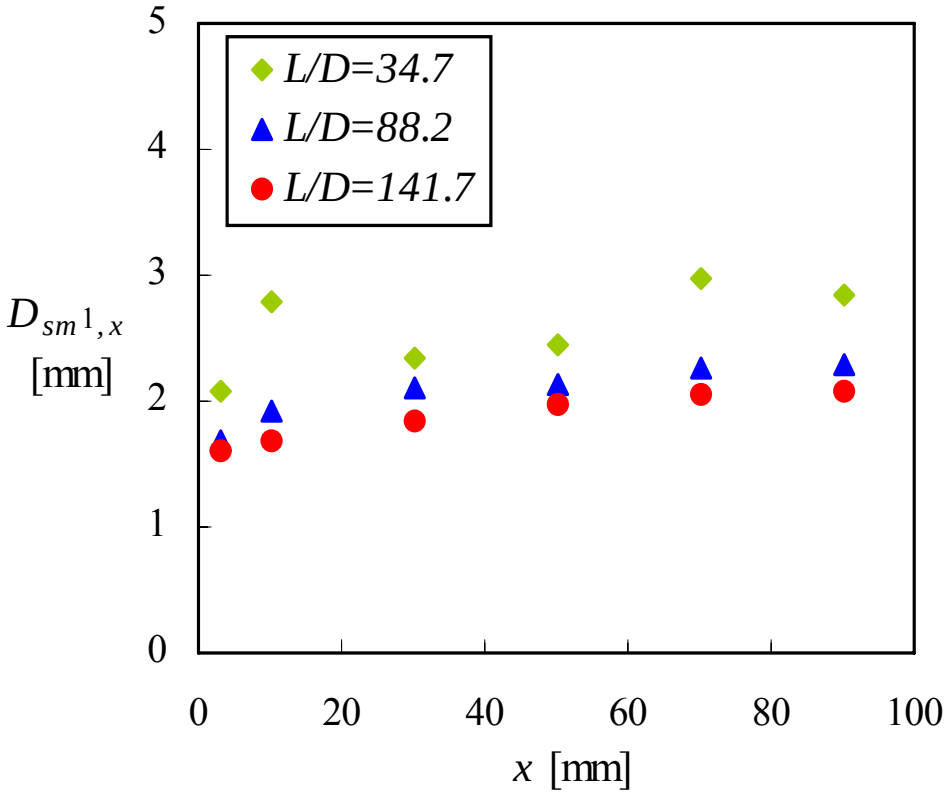

Group 1

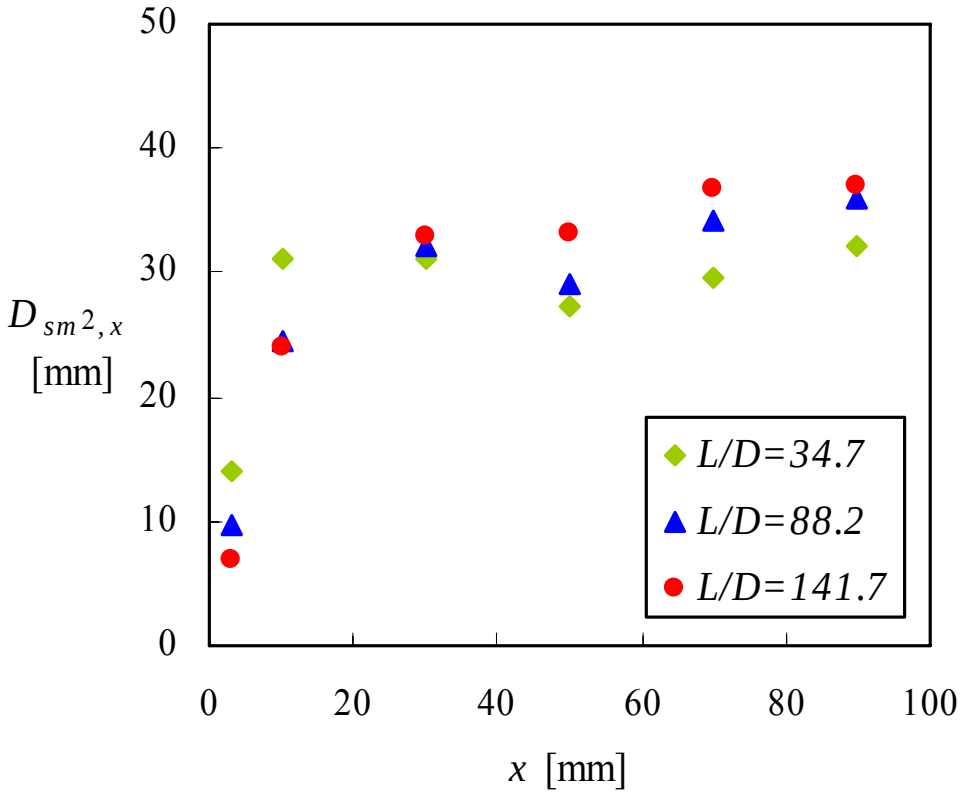

Group 2

$$D_{sm} = \frac{6\alpha}{a_i}$$

Data of Run 12 : Bubble Frequency

(j_f = 2.84 and j_{g0} = 1.0 m/s)

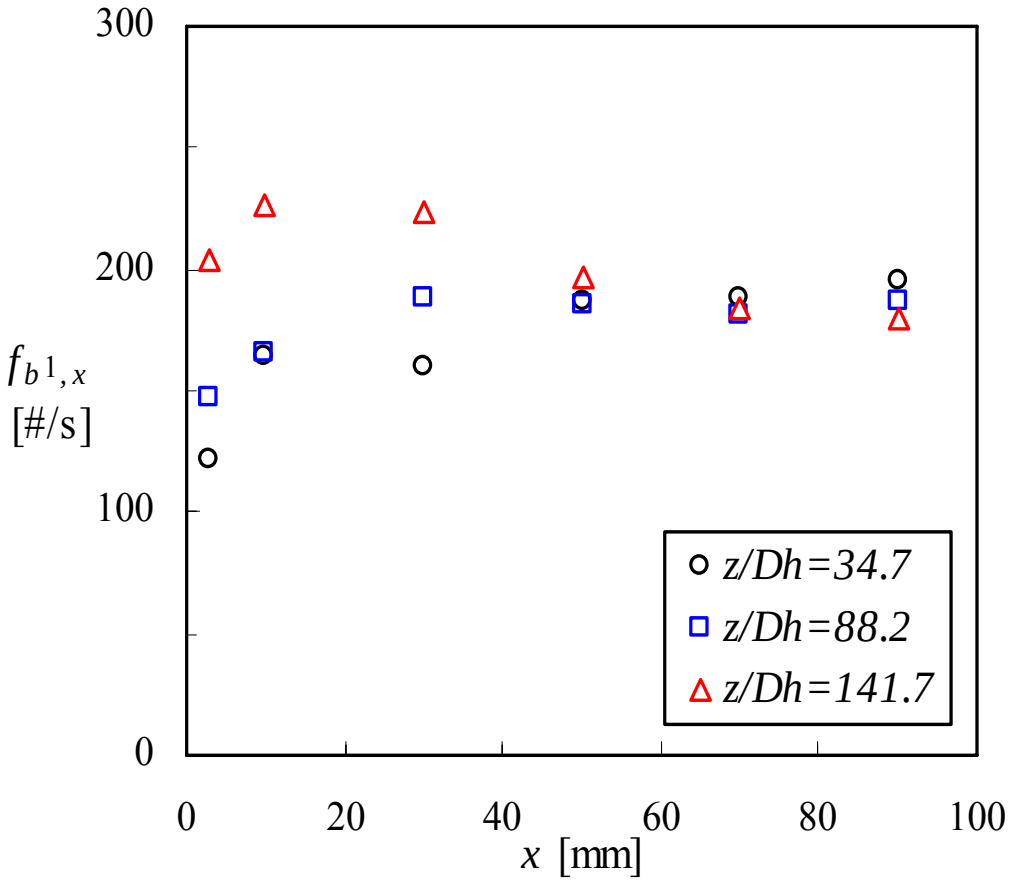

(a) Group 1 bubbles

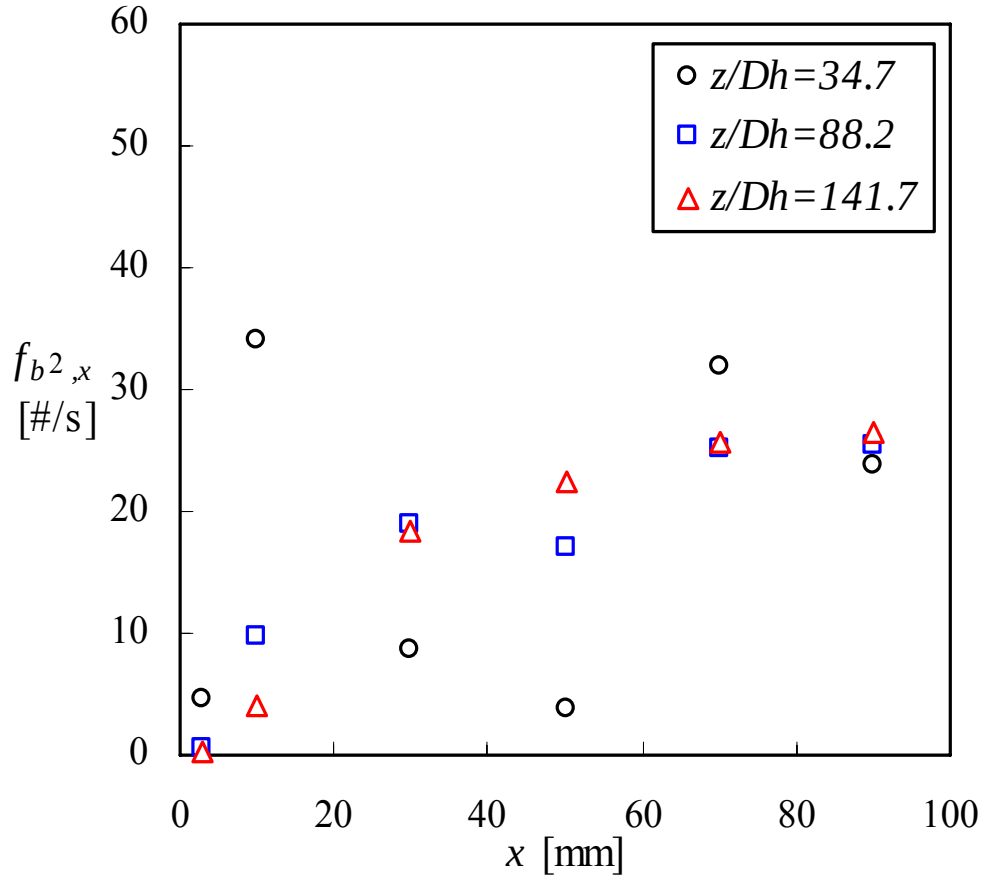

(b) Group 2 bubbles

Modeling of Interfacial Area Transport

Interfacial Area Transport Equation

- One-Group Interfacial Area Transport Equation (Wu et al., '98; Kim, '99; Ishii et al., '02)
  - Small Bubble Interactions Modeled: No Large Bubble Interactions Modeled
  - Applicable to Bubbly Flow: Cannot Correctly Predict Cap-bubbly, Slug, and Churn-turbulent Flows
  - Good Agreement between Experimental Data and Model Predictions

- Substantial Differences of Fluid Particle in
  - Size and Shape
    - Spherical, Distorted, Cap, Slug, and Churn-turbulent Bubbles
  - Transport Phenomena
    - Drag Force
    - Particle Interaction Mechanisms
- Multi-group Approach: Two-group (Fu, '01; Sun, '01; Smith, '02)
  - Group 1: Spherical and Distorted Bubbles
  - Group 2: Cap, Slug, and Churn-turbulent Bubbles

Interfacial Area Transport Equation
Theoretical Foundation

- Boltzmann Transport Equation: Number Transport Eq.

$$\frac{\partial f}{\partial t}+\frac{\partial}{\partial V}\left(f\frac{\mathrm{d}V}{\mathrm{d}t}\right)+\nabla\cdot(f\vec{v})+\nabla_{\vec{v}}\cdot\left(\vec{F}f\right)=\sum_j S_j+S_{\mathrm{ph}}$$

- Interfacial Area Transport Equation

$$\int_{V_{\min}}^{V_{\max}}\left[\frac{\partial fA_i}{\partial t}+\nabla\cdot(fA_i\vec{v})+A_i\frac{\partial}{\partial V}\left(f\dot{V}\right)\right]\mathrm{d}V=\int_{V_{\min}}^{V_{\max}}\left[\sum_j S_jA_i+S_{\mathrm{ph}}A_i\right]\mathrm{d}V$$

$$\Rightarrow\quad \frac{\partial a_i}{\partial t}+\nabla\cdot(a_i\vec{v}_i)-\frac{2}{3}\left(\frac{a_i}{\alpha}\right)\left(\frac{\partial\alpha}{\partial t}+\nabla\cdot\alpha\vec{v}_g-\eta_{ph}\right)=\int_{V_{\min}}^{V_{\max}}\left[\sum_j S_jA_i+S_{\mathrm{ph}}A_i\right]\mathrm{d}V$$

$$n=\int_V f\mathrm{d}V;\quad \alpha=\int_V fV\mathrm{d}V;\quad a_i=\int_V fA_i\mathrm{d}V$$

$$R_j=\int_V S_j\mathrm{d}V;\quad \eta_j=\int_V S_jV\mathrm{d}V;\quad \phi_j=\int_V S_jA_i\mathrm{d}V$$

Two-group IAC Transport Equation

- One-group (Wu et al., '98; Kim, '99)

$$\frac{\partial a_i}{\partial t} + \nabla \cdot \left(a_i \vec{v}_i\right) = \frac{2a_{i1}}{3\alpha_1}\left[\frac{\partial \alpha_1}{\partial t} + \nabla \cdot \left(\alpha_1 \vec{v}_{g1}\right) - \eta_{\mathrm{ph1}}\right] + \sum_j \phi_j + \phi_{\mathrm{ph}}$$

- Two-group (Fu, '01; Sun, '01; Smith, '02)

$$\frac{\partial a_{i1}}{\partial t} + \nabla \cdot \left(a_{i1} \vec{v}_{i1}\right) = \left(\frac{2}{3} - CD_{c1}^{*\,2}\right)\frac{a_{i1}}{\alpha_1}\left[\frac{\partial \alpha_1}{\partial t} + \nabla \cdot \left(\alpha_1 \vec{v}_{g1}\right) - \eta_{\mathrm{ph1}}\right] + \sum_j \phi_{j,1} + \phi_{\mathrm{ph1}}$$

$$\frac{\partial a_{i2}}{\partial t} + \nabla \cdot \left(a_{i2} \vec{v}_{i2}\right) = \frac{2}{3}\frac{a_{i2}}{\alpha_2}\left[\frac{\partial \alpha_2}{\partial t} + \nabla \cdot \left(\alpha_2 \vec{v}_{g2}\right)\right]$$

$$+CD_{c1}^{*\,2}\frac{a_{i1}}{\alpha_1}\left[\frac{\partial \alpha_1}{\partial t} + \nabla \cdot \left(\alpha_1 \vec{v}_{g1}\right) - \eta_{\mathrm{ph1}}\right] + \sum_j \phi_{j,2} + \phi_{\mathrm{ph2}}$$

where,

$$\phi_j \equiv \int_V S_j A_i \,\mathrm{d}V, \qquad D_{c1}^{*} = \left(\frac{D_c}{D_{sm1}}\right), \qquad C = \frac{f_c V_c}{n_1}$$

Demonstration of Inter-group Transfer Coefficient C

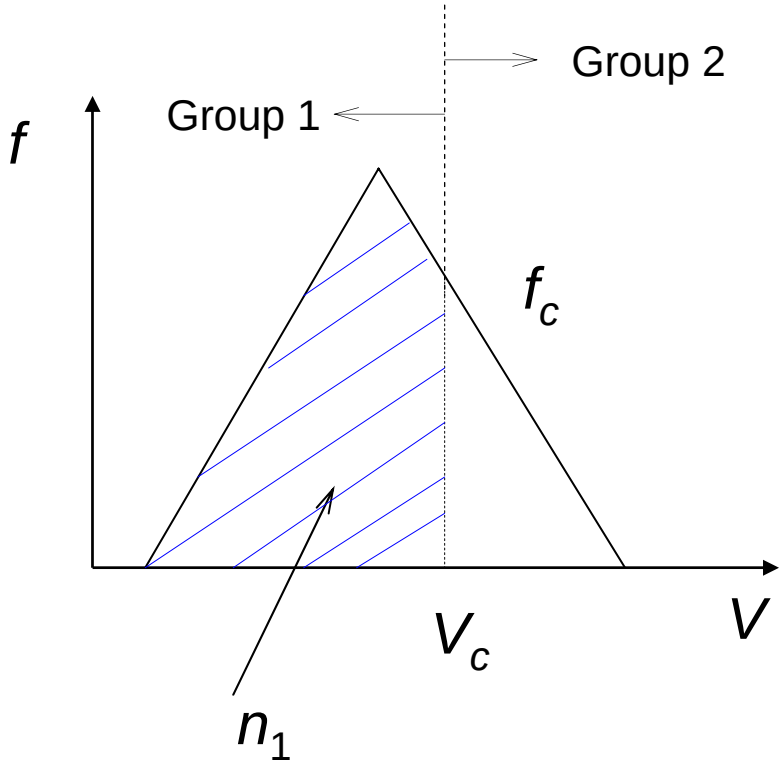

$$C = \frac{f_c V_c}{n_1}$$

Two-group Void Fraction Transport Equation

One-group:

$$\frac{\partial \alpha \rho_g}{\partial t} + \nabla \cdot \left(\alpha \rho_g \vec{v}_g \right) = \Gamma_g$$

Two-group:

$$\frac{\partial \left(\alpha_1 \rho_g \right)}{\partial t} + \nabla \cdot \left(\alpha_1 \rho_g \vec{v}_{g1} \right) = \Gamma_{g1} - \Delta \dot{m}_{12}$$

$$\frac{\partial \left(\alpha_2 \rho_g \right)}{\partial t} + \nabla \cdot \left(\alpha_2 \rho_g \vec{v}_{g2} \right) = \Gamma_{g2} + \Delta \dot{m}_{12}$$

$$\Delta \dot{m}_{12} = \rho_g \left[\left(\sum_j \eta_{j,12} - \sum_j \eta_{j,21} \right) + CD_{c1}^{*\,3} \left(\frac{\partial \alpha_1}{\partial t} + \nabla \cdot \left(\alpha_1 \vec{v}_{g1} \right) - \eta_{\mathrm{ph1}} \right) \right]$$

$$\eta_j \equiv \int_V S_j V \mathrm{d}\, V$$

$$\alpha = \alpha_1 + \alpha_2, \quad \Gamma_g = \Gamma_{g1} + \Gamma_{g2}, \quad \vec{v}_g = \frac{\alpha_1 \vec{v}_{g1} + \alpha_2 \vec{v}_{g2}}{\alpha_1 + \alpha_2}$$

Modeling of Two-group Bubble Interaction Mechanisms

- Bubble Coalescence
  - Random Collision
  - Wake Entrainment
- Bubble Disintegration
  - Surface Instability
  - Shearing-off
  - Turbulent Impact

Sun et al., Nuclear Engineering and Design, 230(1-3), 3-26, 2004

Fluid Particle Interaction Mechanisms

- Coalescence Mechanisms (Sinks)
  - Turbulence induced random collision: *Howarth ('64), Kirpatrick & Lockett ('74), Thomas ('81), Prince & Blanch ('90), Stewart ('95), Kim ('99), etc.*
  - Wake induced entrainment: *Crabtree & Bridgwater ('71), Nevers & Wu ('71), Otake et al. ('76), Tsuchiya et al. ('89 & '96), Stewart et al. ('93), etc.*
- Disintegration Mechanisms (Sources)
  - Impact of turbulent eddies: *Hinze ('55), Sevik & Park ('73), Coulalogou & Tavlarides ('77), Kitcha & Kojasoy ('89), Prince & Blanch ('90), Duinveld ('93), Wu et al. ('98), Kim ('99), etc.*
  - Shearing off at the rim of large bubbles: *Thomson & Newell (1885), Collins ('67), Wegener et al. ('71), Nickens & Yannitell ('87), Kim ('99), etc.*
  - Surface instability: *Taylor ('34), Ishii & Kojasoy ('84), Miller et al. ('93)*
  - Laminar shear in viscous fluid: *Hinze ('55), etc.*

Images of Wake Entrainment
(500 Frames/s)

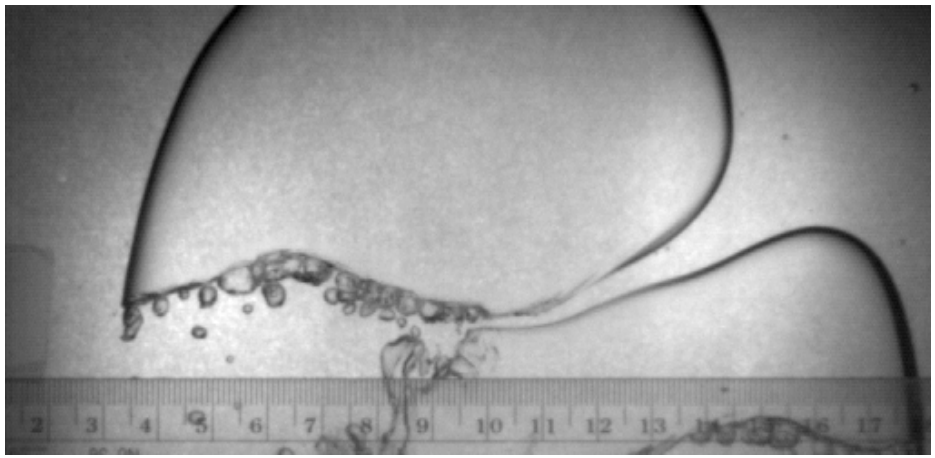

t = 0

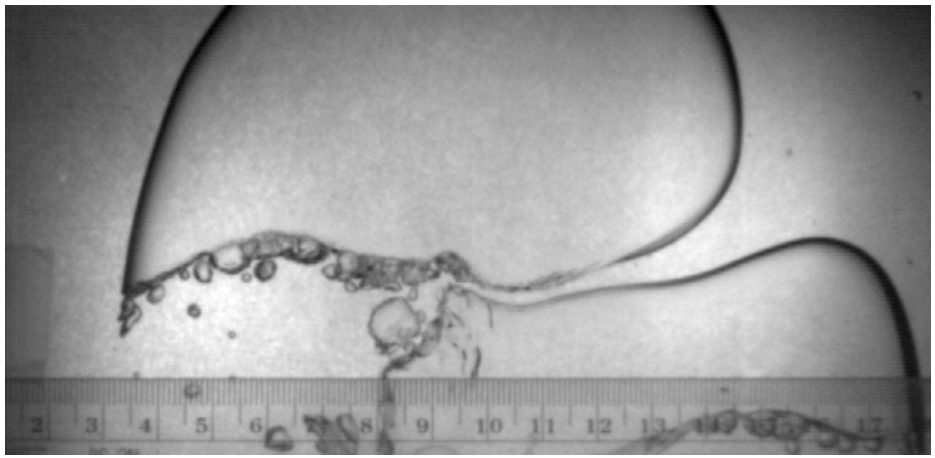

t = 8 ms

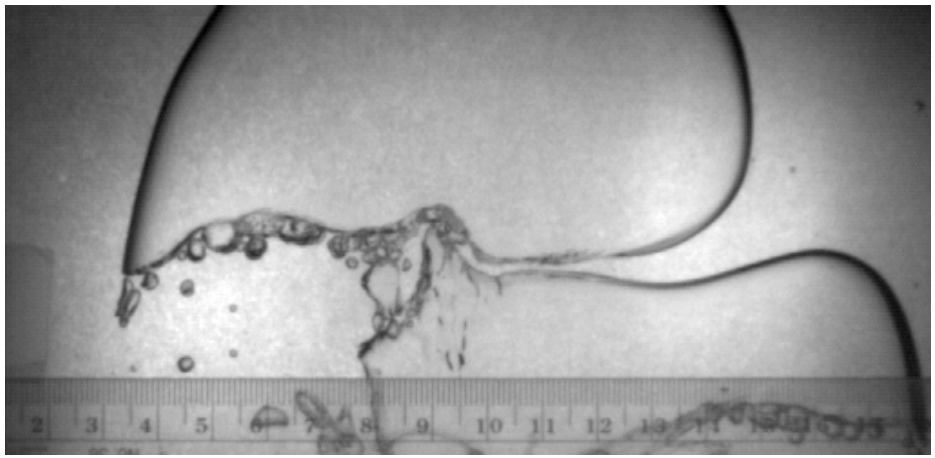

t = 16 ms

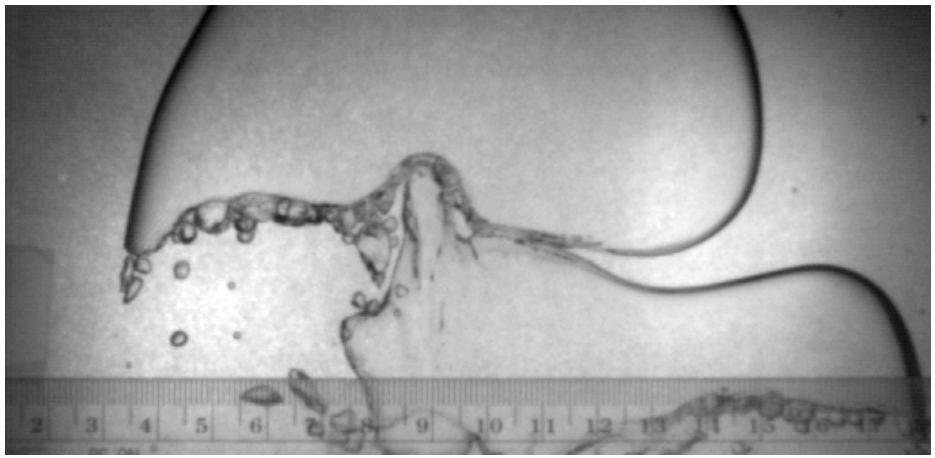

t = 24 ms

Images of Wake Entrainment (Cont'd)
(500 Frames/s)

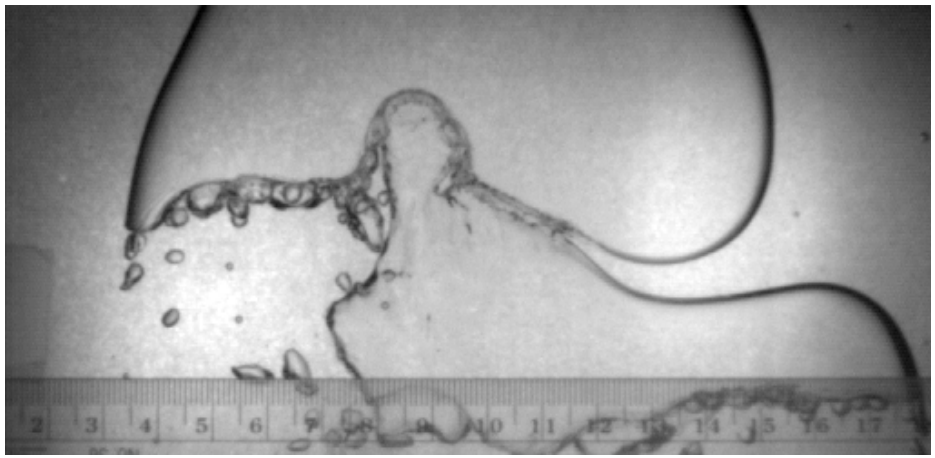

t = 32 ms

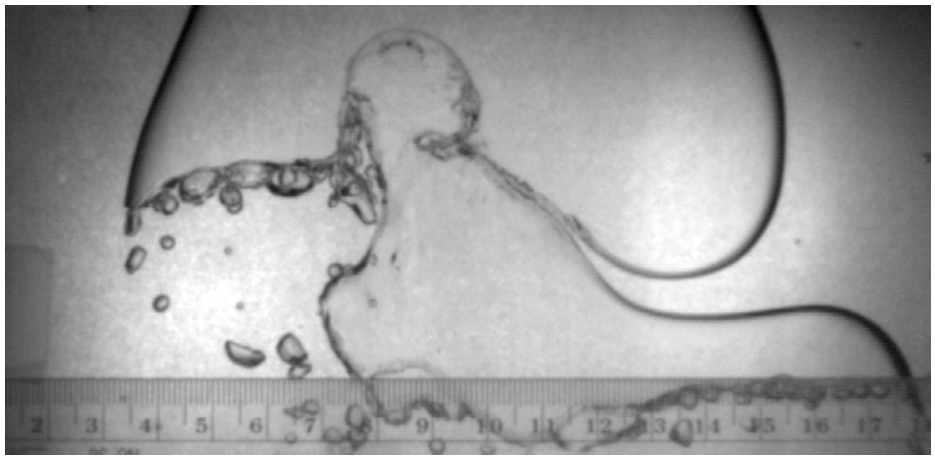

t = 40 ms

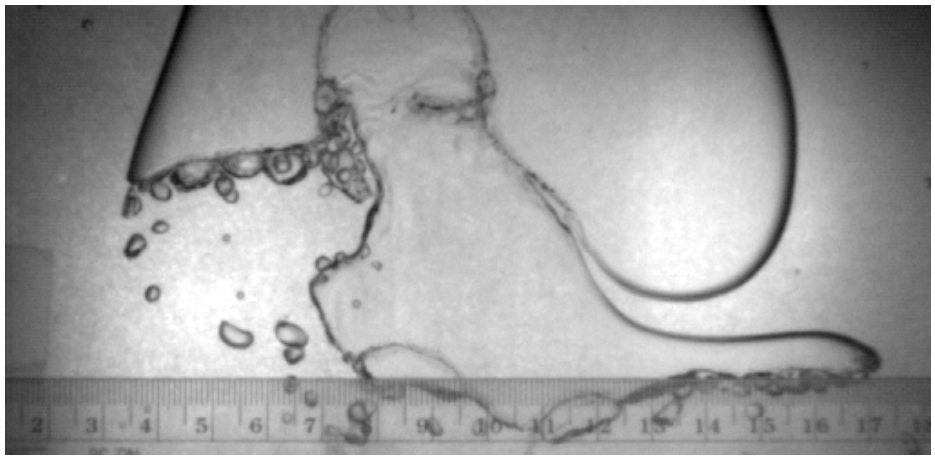

t = 48 ms

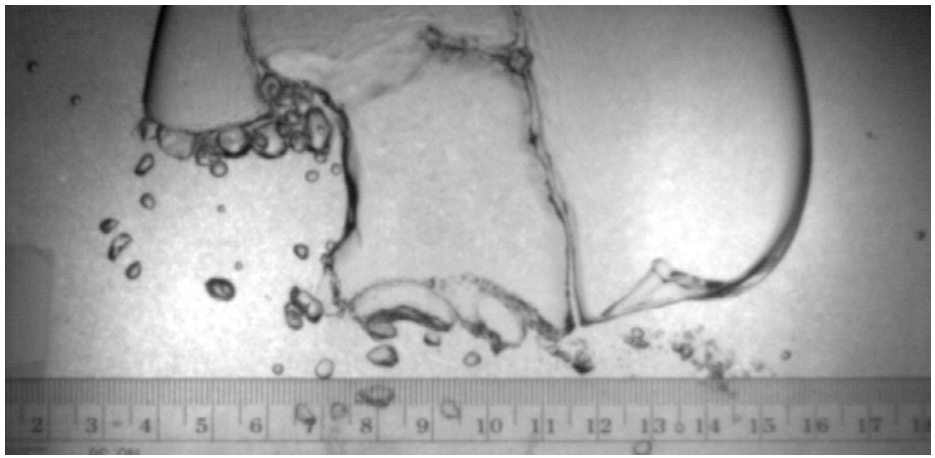

t = 76 ms

Images of Turbulent Impact
(500 Frames/s)

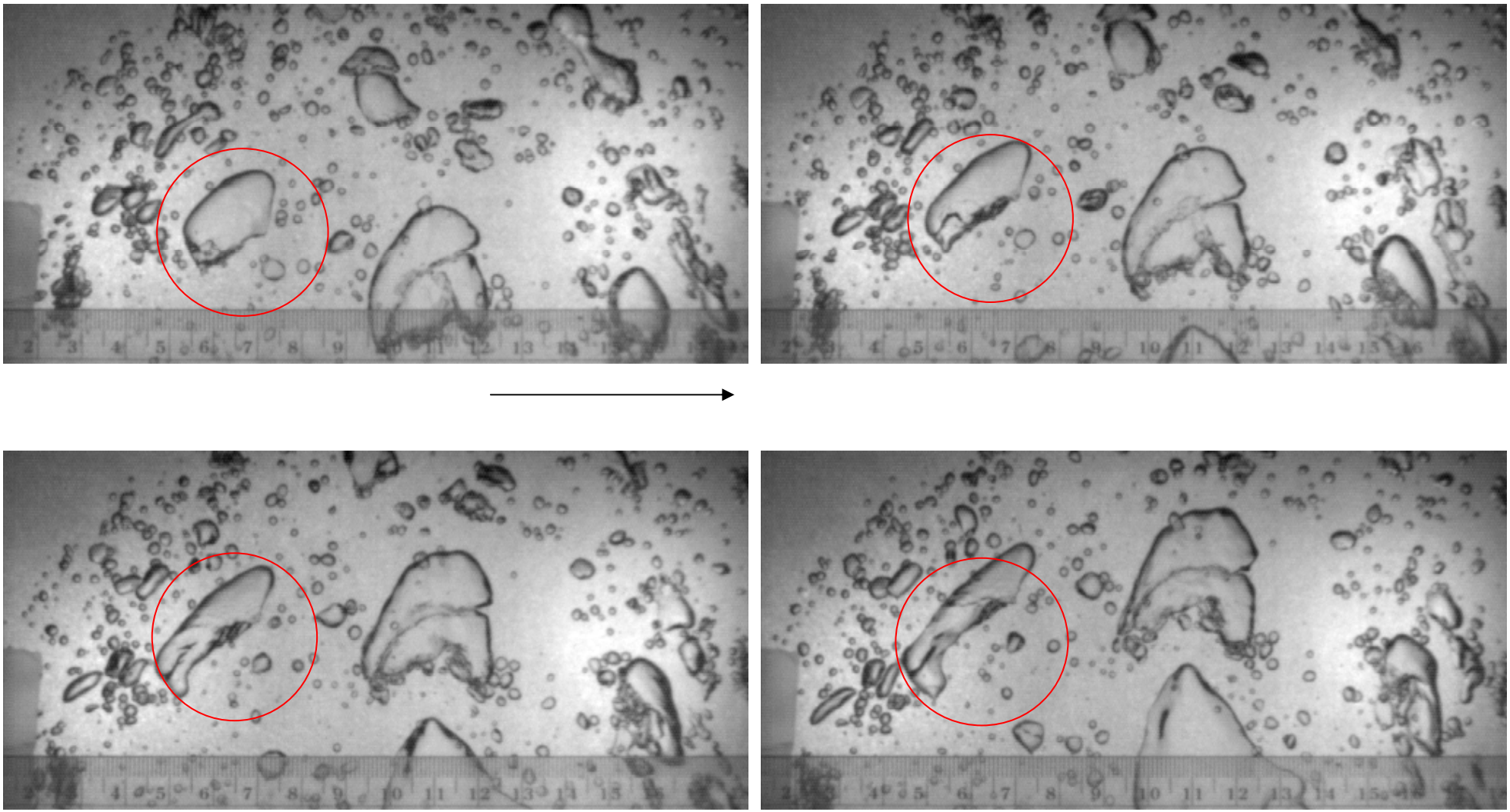

time

Images of Turbulent Impact (Cont'd)
(500 Frames/s)

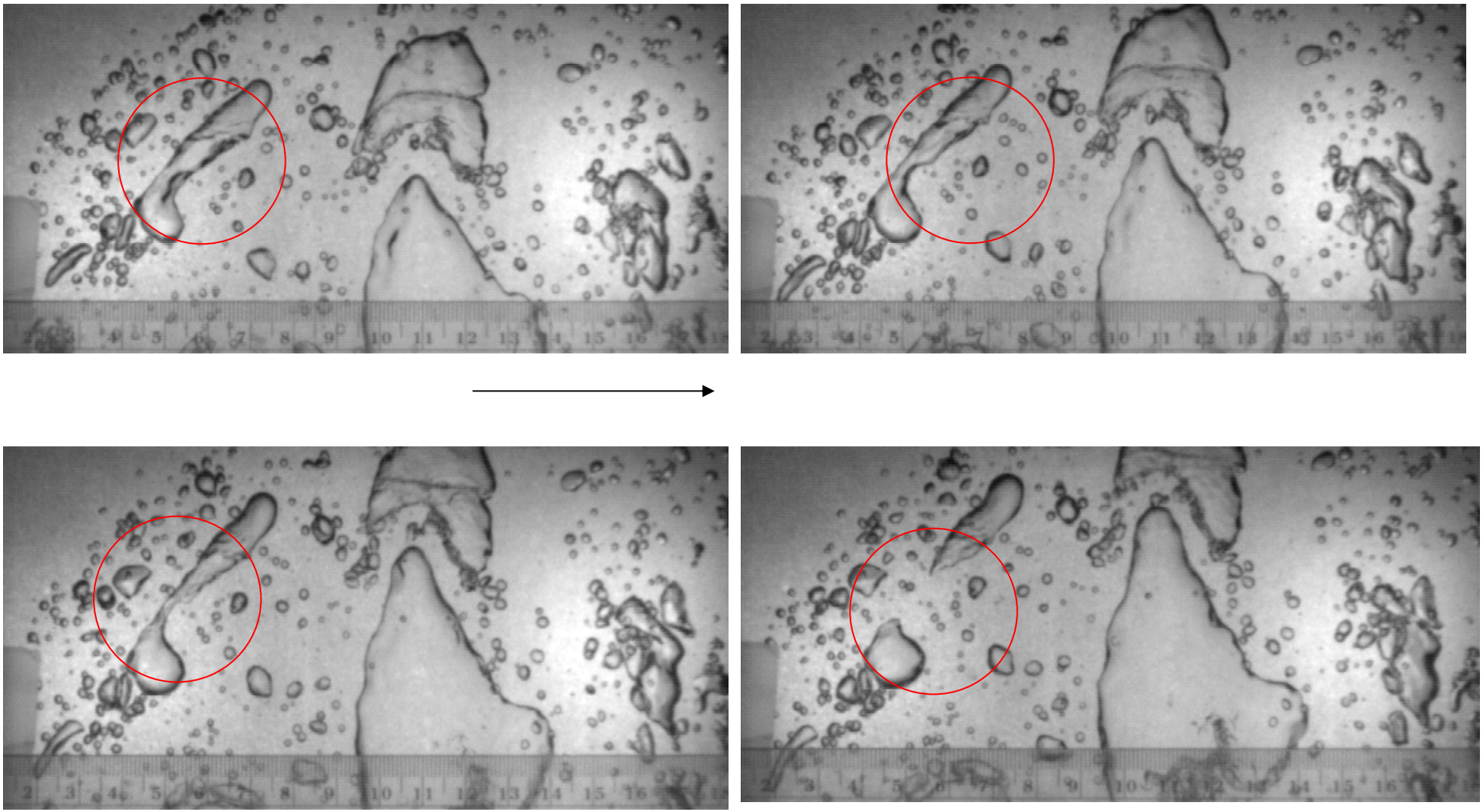

time

Major Two-Group Bubble Interaction Mechanisms

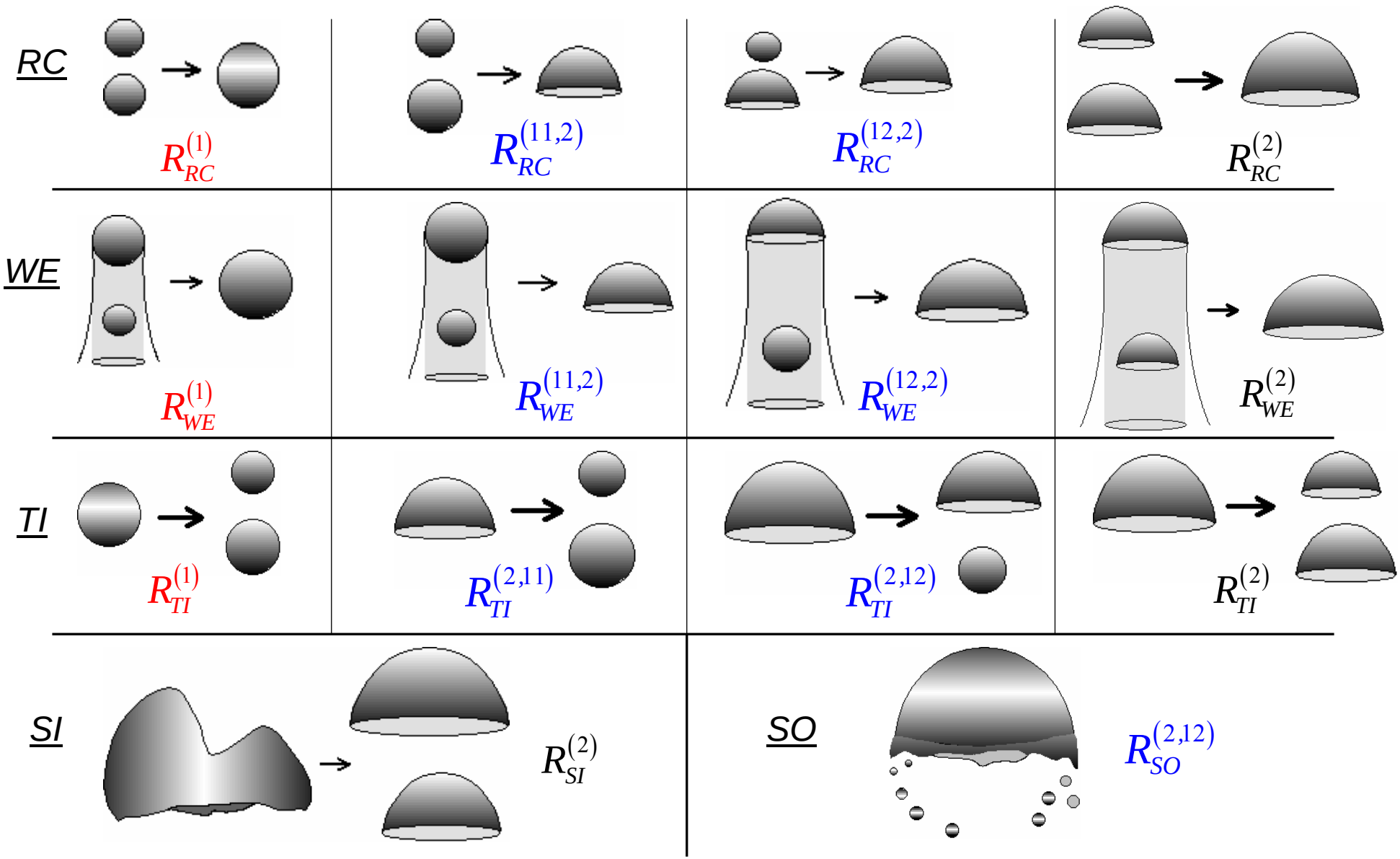

Experimental Flow Conditions

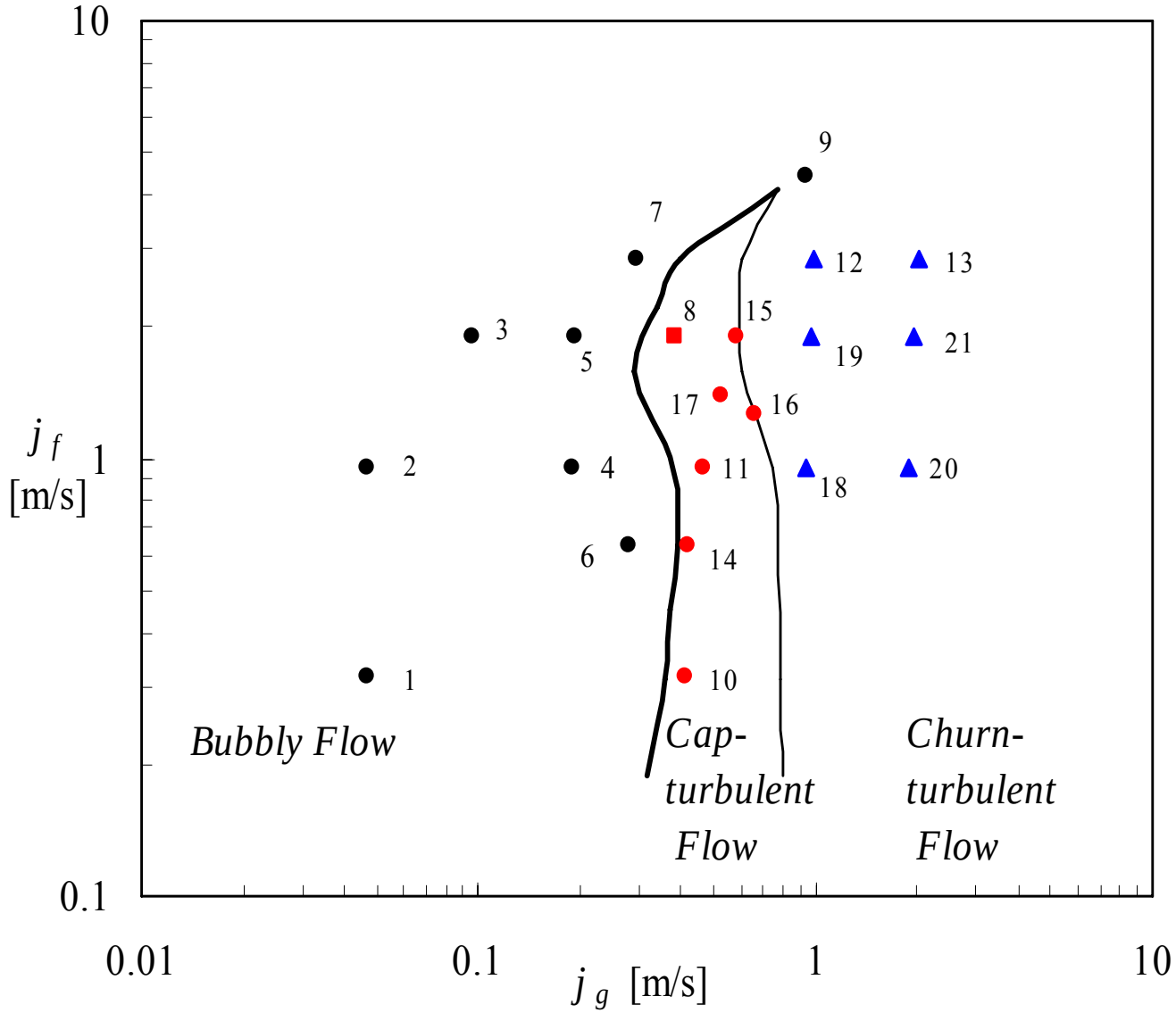

1-D Evaluation Results for Run 9

(Highly Turbulent Dispersed Bubbly Flow)

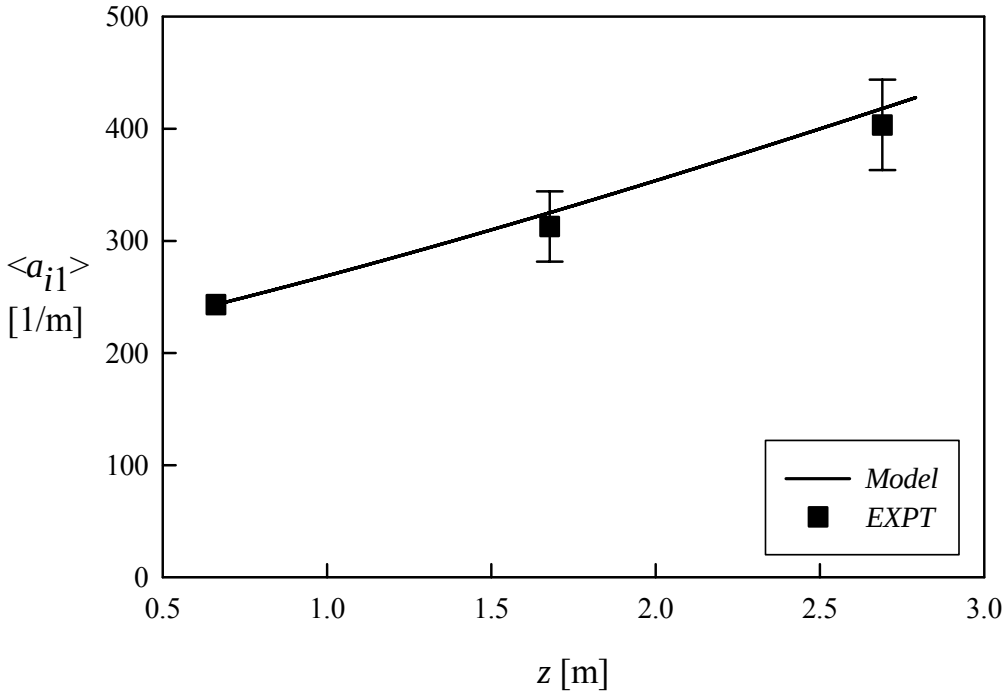

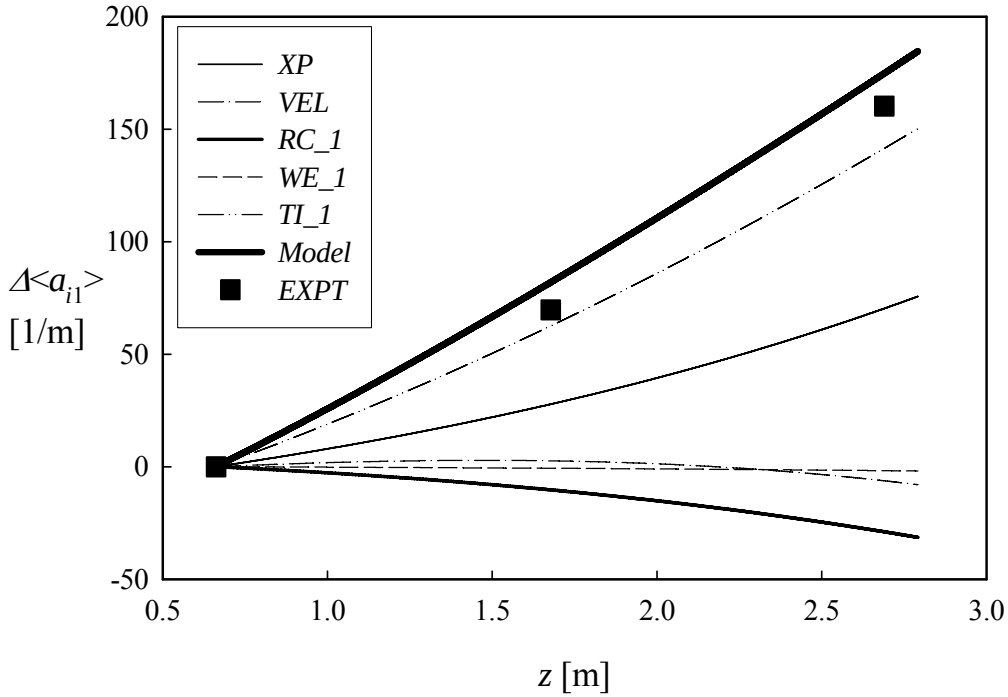

Error Bar: ±10%

Evaluation Results of $<a_i>$ and $<\alpha>$ for Run 12

(Churn-turbulent Flow, Highly Turbulent)

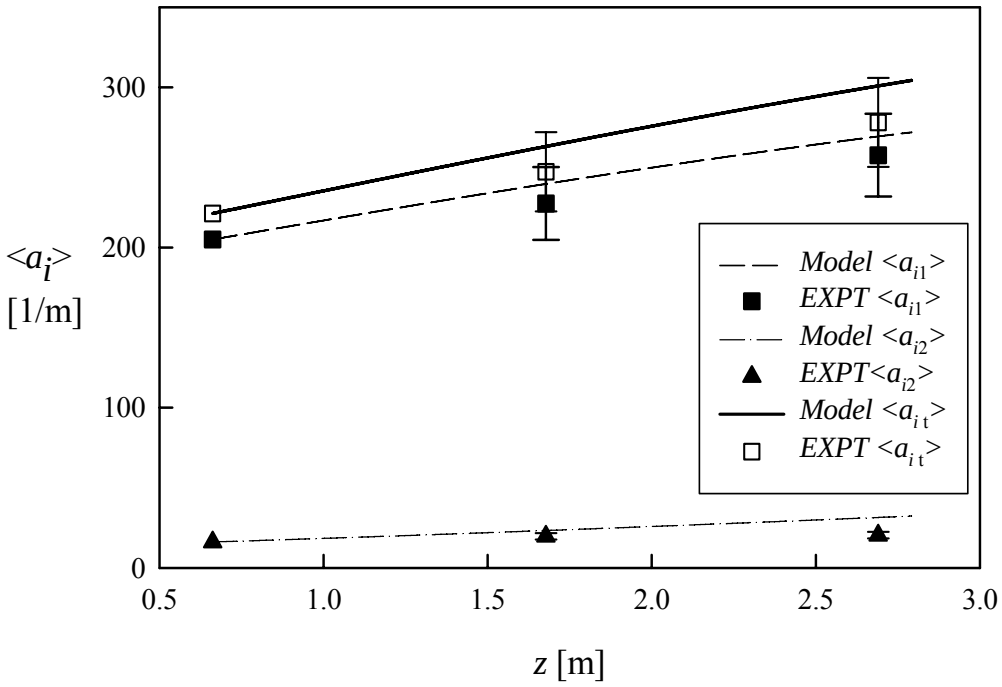

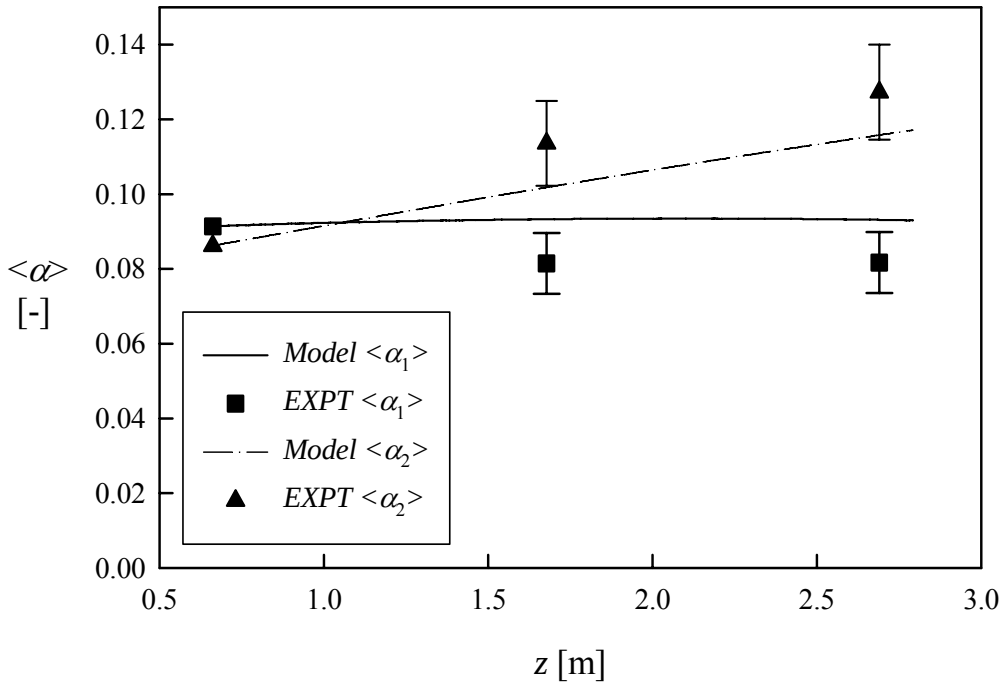

Error Bar: ±10%

Implementation of One-group IATE into FLUENT

- Implementation Strategy
- Some Preliminary Results

One-group IATE

- Spherical or Distorted (Small) Bubbles

$$\frac{\partial a_i}{\partial t} + \nabla \cdot \left(a_i \vec{v}_i \right) \cong \frac{2a_i}{3\alpha} \left[\frac{\partial \alpha}{\partial t} + \nabla \cdot \left(\alpha \vec{v}_g \right) \right] + \frac{1}{3\psi} \left(\frac{\alpha}{a_i} \right)^2 \sum_j R_j + \pi D_{bc}^2 R_{ph} \left[1 - \frac{2}{3} \left(\frac{D_{bc}}{D_{sm}} \right) \right]$$

Gas expansion

Phase-change mechanism: Nucleation and condensation

For adiabatic air-water flows

$$\frac{\partial a_i}{\partial t} + \nabla \cdot \left(a_i \vec{v}_i \right) \cong \frac{2a_i}{3\alpha} \left[\frac{\partial \alpha}{\partial t} + \nabla \cdot \left(\alpha \vec{v}_g \right) \right] + \frac{1}{3\psi} \left(\frac{\alpha}{a_i} \right)^2 \sum_j R_j$$

Source/sink due to bubble interactions

Models from Ishii et al., '02

Bubble Interaction Models
(Ishii et al., '02)

- Disintegration due to Impact of Liquid Turbulent Eddies (TI)

$$R_{TI} = \frac{C_{TI}\psi}{6}\left(\frac{\langle a_i \rangle^4}{\langle \alpha \rangle^3}\langle u_t \rangle\right)\sqrt{1-\frac{We_{cr}}{We}}\exp\left(-\frac{We_{cr}}{We}\right)$$

- Coalescence Caused by Wake Entrainment (WE)

$$R_{WE} = -36\psi^2 C_{WE} C_D{}^{1/3}\left(\frac{\langle a_i \rangle^4}{\langle \alpha \rangle^2}\langle u_r \rangle\right)$$

- Coalescence due to Random Collision Driven by Liquid Turbulent Eddies (RC)

$$R_{RC} = -36\psi^2 C_{RC}\frac{\langle a_i \rangle^4 \langle u_t \rangle}{\langle \alpha \rangle^2 \langle \alpha \rangle_{\max}{}^{1/3}\left(\langle \alpha \rangle_{\max}{}^{1/3} - \langle \alpha \rangle^{1/3}\right)}$$

$$\left[1-\exp\left(-\frac{C\langle \alpha \rangle_{\max}{}^{1/3}\langle \alpha \rangle^{1/3}}{\left(\langle \alpha \rangle_{\max}{}^{1/3} - \langle \alpha \rangle^{1/3}\right)}\right)\right]$$

Implementation Approach

- The Current FLUENT Code Does not Dynamically Model the Evolution of the Bubble Size

- To Implement Steady-state One-group IATE for Adiabatic Bubbly Flows:
  - Specify the Interfacial Area Concentration as a User-defined Function (UDF) in the Gas/Vapor Domain
  - The Default Transport Equation for the UDF is Solved by FLUENT as

$$\frac{\partial\left(\alpha\rho_g a_i\right)}{\partial t} + \nabla\cdot\left(\alpha\rho_g\vec{v}_g a_i - \alpha\Gamma_g\nabla a_i\right) = S_g(a_i)$$

- The One-group IATE

$$\frac{\partial a_i}{\partial t} + \nabla\cdot\left(a_i\vec{v}_i\right) \cong \frac{2a_i}{3\alpha}\left[\frac{\partial\alpha}{\partial t} + \nabla\cdot\left(\alpha\vec{v}_g\right)\right] + \frac{1}{3\psi}\left(\frac{\alpha}{a_i}\right)^2\sum_j R_j$$

$$\vec{v}_i \approx \vec{v}_g$$

Implementation Approach (Cont'd)

- The Default Transport Equation for the UDF a_i:

$$\nabla \cdot (\alpha \rho_g \vec{v}_g a_i - \alpha \Gamma_g \nabla a_i) = S_g(a_i)$$

- The One-group IATE:

$$\nabla \cdot \left(a_i \vec{v}_g\right) \cong \frac{2a_i}{3\alpha}\left(\alpha \vec{v}_g\right) + \frac{1}{3\psi}\left(\frac{\alpha}{a_i}\right)^2 \sum_j R_j$$

$$\Rightarrow \alpha \rho_g \nabla \cdot \left(a_i \vec{v}_g\right) \cong \frac{2a_i \rho_g}{3}\left(\alpha \vec{v}_g\right) + \frac{1}{3\psi}\left(\frac{\rho_g \alpha^3}{a_i^2}\right) \sum_j R_j$$

- Therefore:

$$\Gamma_g = 0$$

$$S_g(a_i) = -\left(\alpha a_i \rho_g\right) \nabla \cdot \vec{v}_g + \frac{2a_i \rho_g}{3} \nabla \cdot \left(\alpha \vec{v}_g\right) + \frac{\rho_g \alpha^3}{3\psi a_i^2}\left(R_{TI} + R_{WE} + R_{RC}\right)$$

Momentum Eq.: Gas Phase

- In Fluent

$$\frac{\partial}{\partial t}\left(\alpha\rho_g\vec{v}_g\right)+\nabla\cdot\left(\alpha\rho_g\vec{v}_g\vec{v}_g\right)=-\alpha\nabla p+\alpha\rho_g\vec{g}$$
$$+\alpha\mu_g\left(\nabla\vec{v}_g+\nabla\vec{v}_g{}^{t}\right)+\vec{R}_{fg}+\vec{F}_l+\vec{F}+\vec{F}_{vm}$$

- Steady-state Drag Force

$$\vec{R}_{fg}=f(\mathrm{Re},C_D,D_b,\alpha,\rho_f,\vec{v}_r)$$

$$D_b\approx D_{sm}=\frac{6\alpha}{a_i}$$

$$\vec{R}_{fg}=-\frac{a_i}{8}C_D\rho_f(\vec{v}_g-\vec{v}_f)\left|\vec{v}_g-\vec{v}_f\right|$$

- Lift Force

$$\vec{F}_l=-C_l\alpha\rho_f\left(\vec{v}_g-\vec{v}_f\right)\times\left(\nabla\times\vec{v}_f\right)\qquad C_l=0.5$$

Numerical Model (Circular Pipe)

- Air-water Bubbly Flow in a Round Pipe
  - Inner pipe diameter: 50.8 mm
  - Length: 3.06 m
- A Quarter of the Pipe was Modeled
- Working Fluid
  - Liquid: Water (Incompressible Fluid)
  - Gas: Air (Ideal Gas at 297 K)

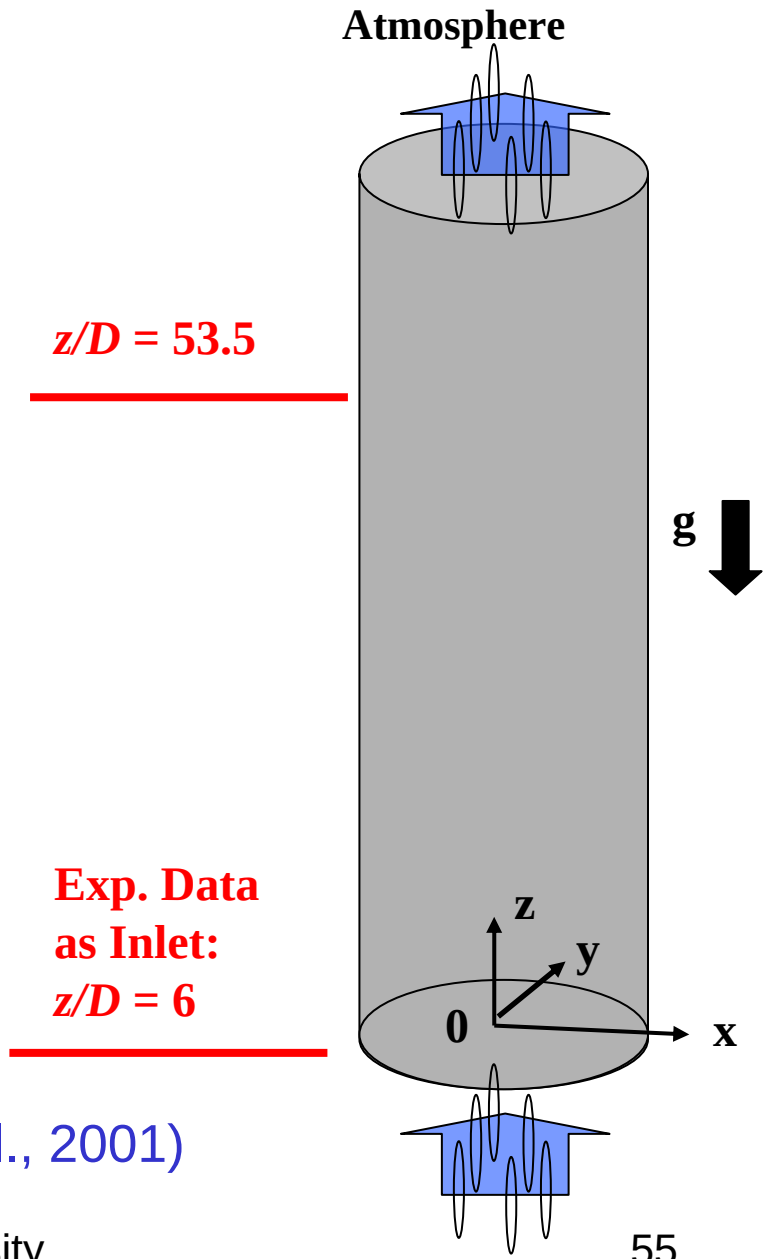

(Hibiki et al., 2001)

Boundary Conditions

- Inlet Boundary Conditions: Experimental Data Measured at Location $z/D = 6$ (Hibiki et al., 2001)

Run #	$\langle j_f \rangle$ (m/s)	$\langle j_g \rangle$ (m/s)	$\langle \alpha \rangle$ (%)
C-1	0.99	0.24	20.3
C-2	0.49	0.13	19.2
C-3	0.49	0.03	4.9
C-4	0.99	0.32	23.1

- Outlet: Atmospheric Pressure

Unstructured Meshes

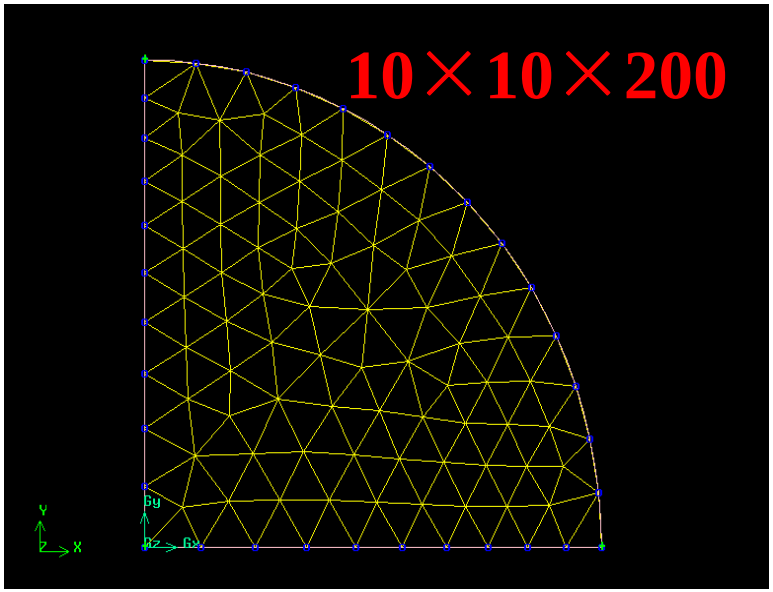

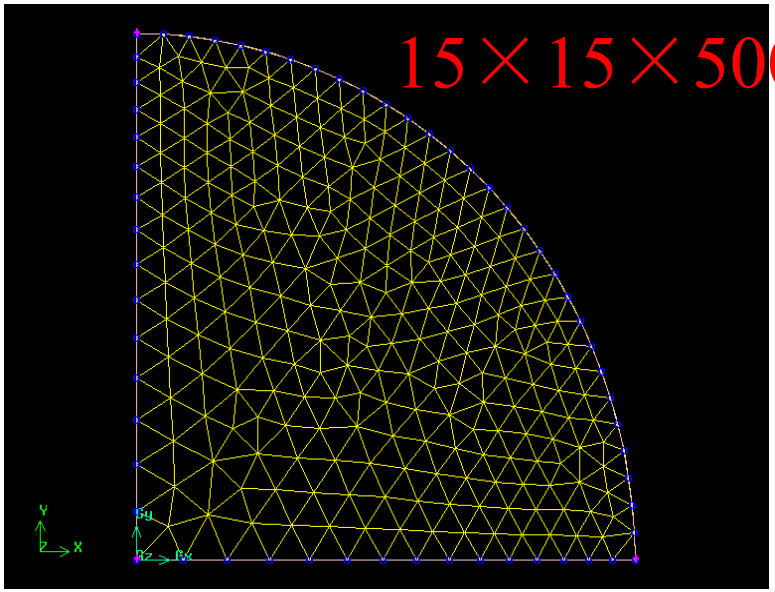

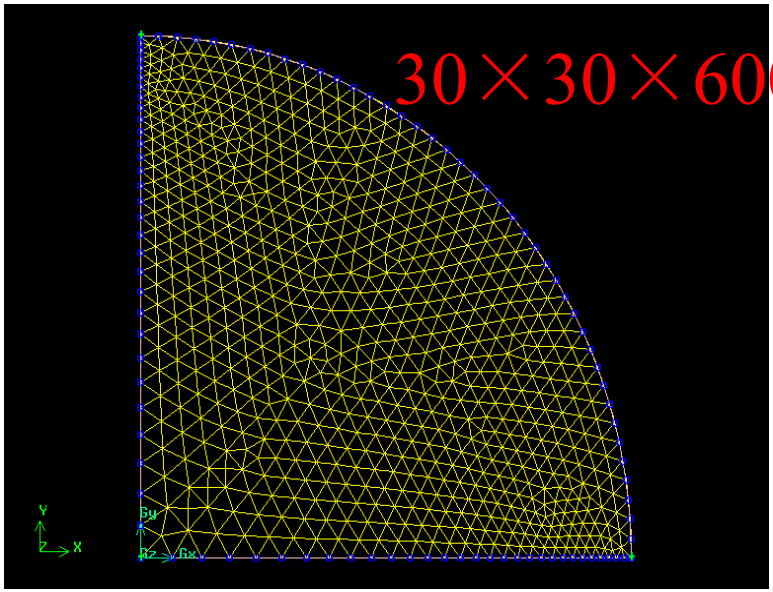

Mesh Sensitivity: Run C-1 IAC

$(j_f = 0.98 \text{ and } j_g = 0.24 \text{ m/s})$

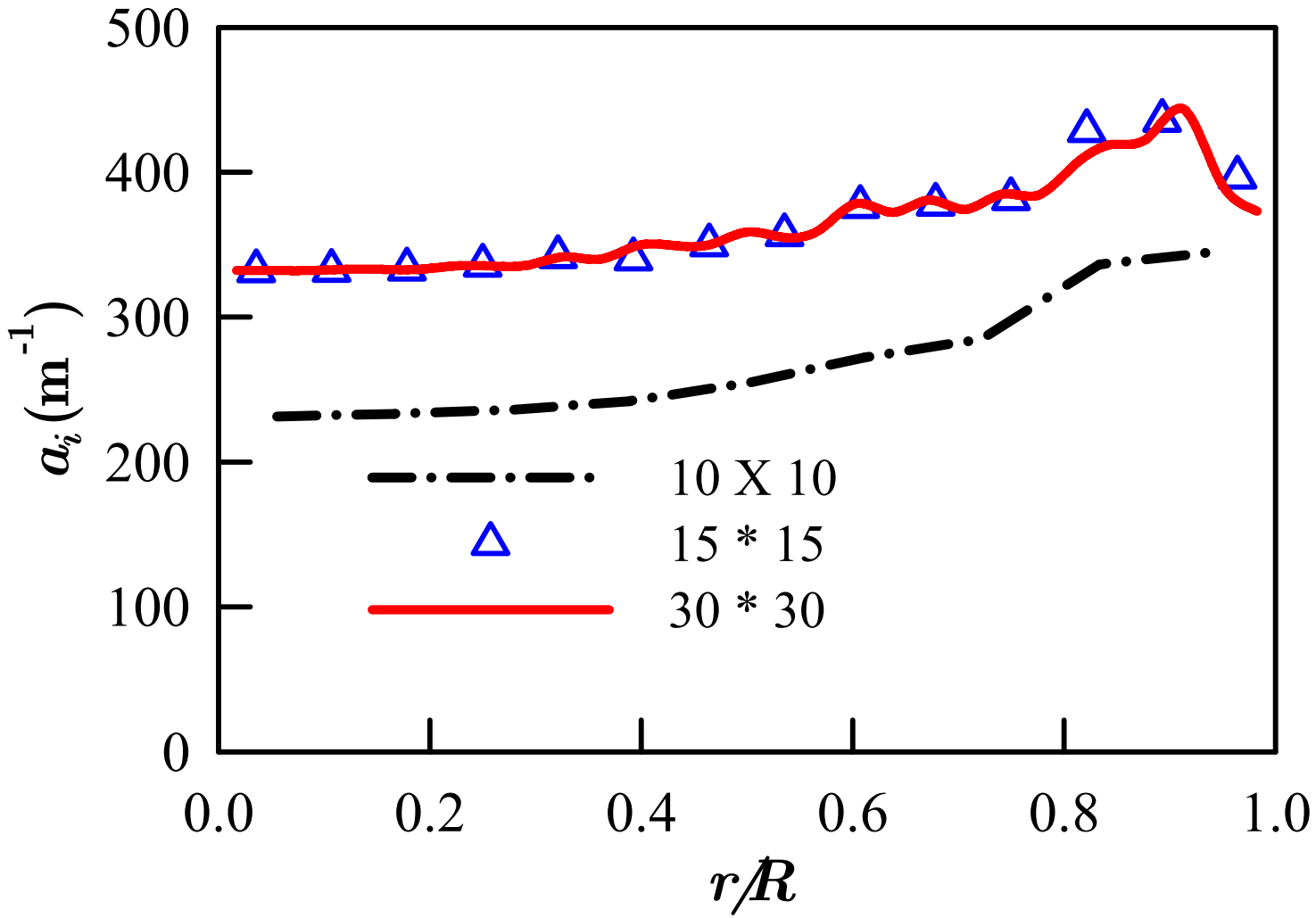

Interfacial Area Concentration

Comparison: Run C-2 VF

$(j_f = 0.49 \text{ and } j_g = 0.13 \text{ m/s})$

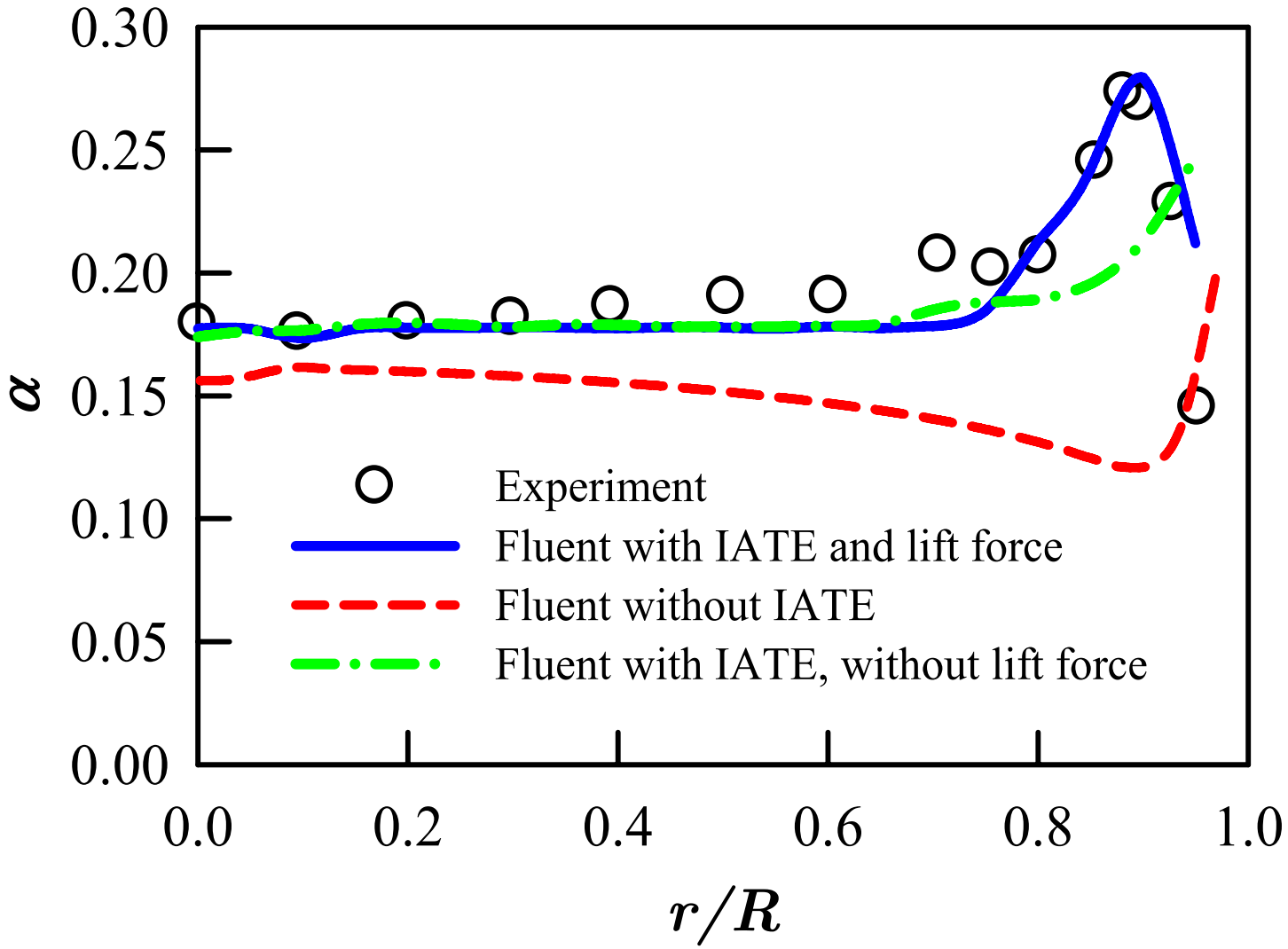

Void Fraction

Comparison: Run C-2 IAC

$(j_f = 0.49 \text{ and } j_g = 0.13 \text{ m/s})$

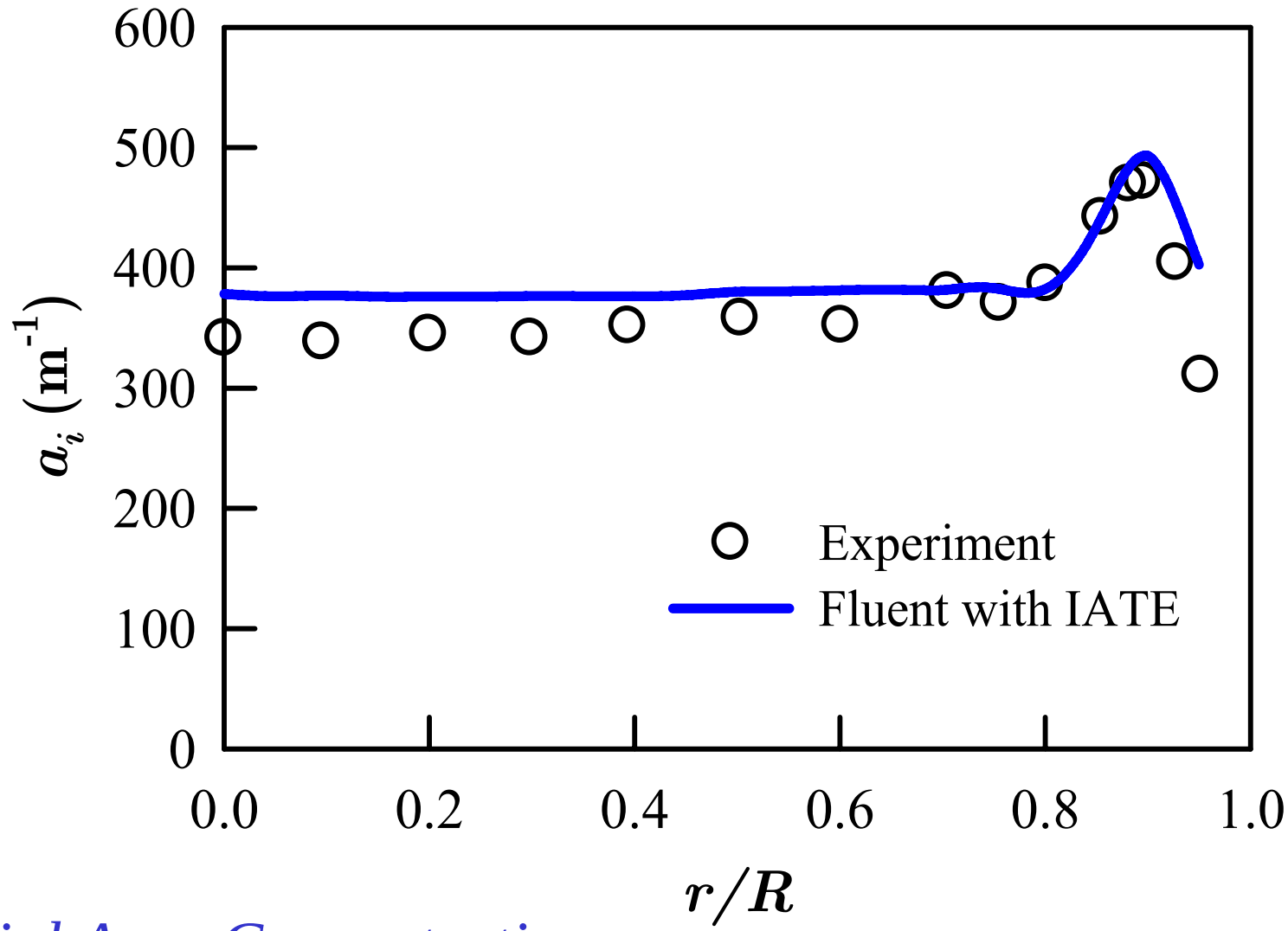

Interfacial Area Concentration

Comparison: Run C-2 D_{sm}

$(j_f = 0.49 \text{ and } j_g = 0.13 \text{ m/s})$

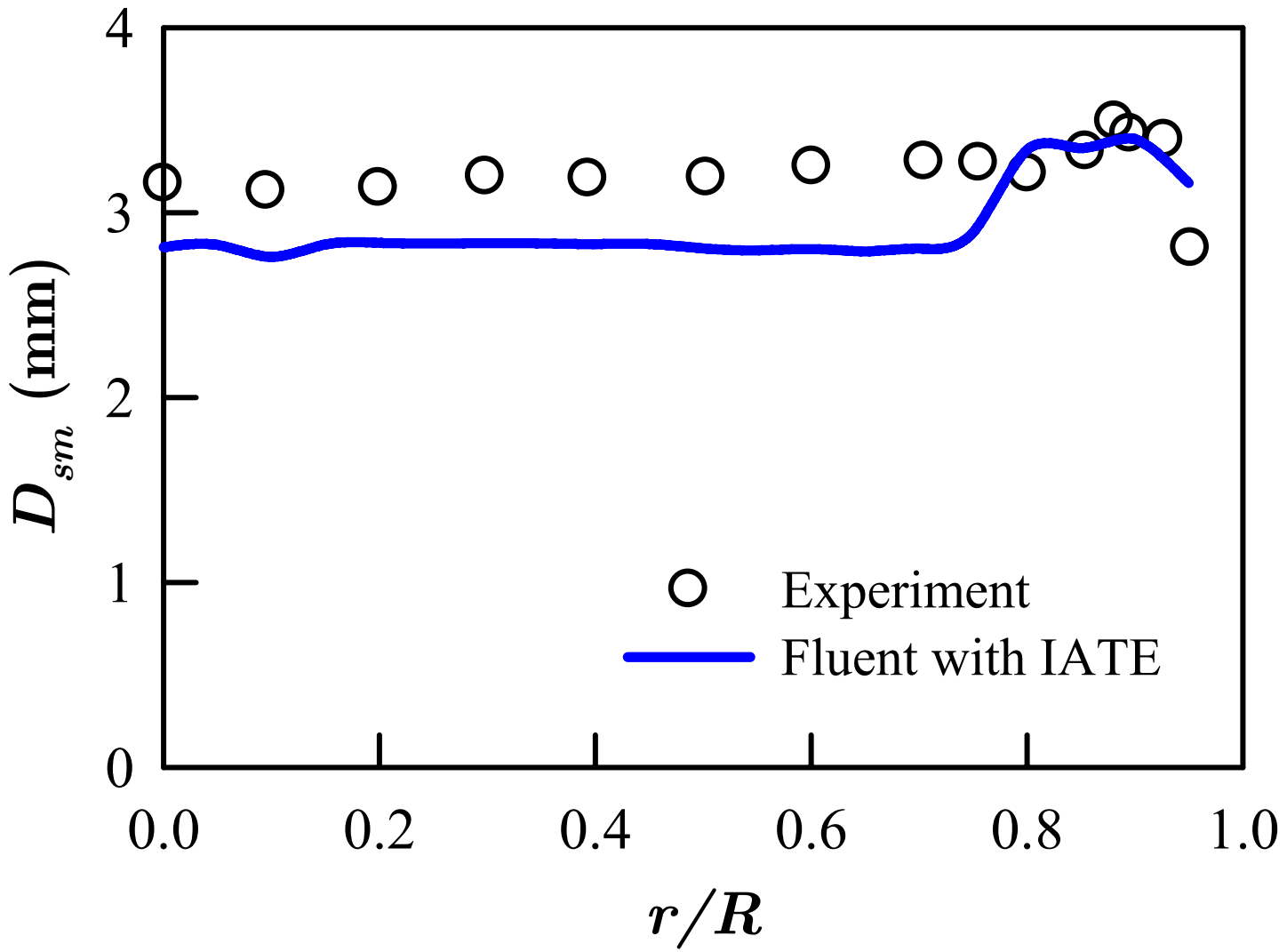

Bubble Sauter Mean Diameter

Comparison: Run C-3 VF

$(j_f = 0.49 \text{ and } j_g = 0.03 \text{ m/s})$

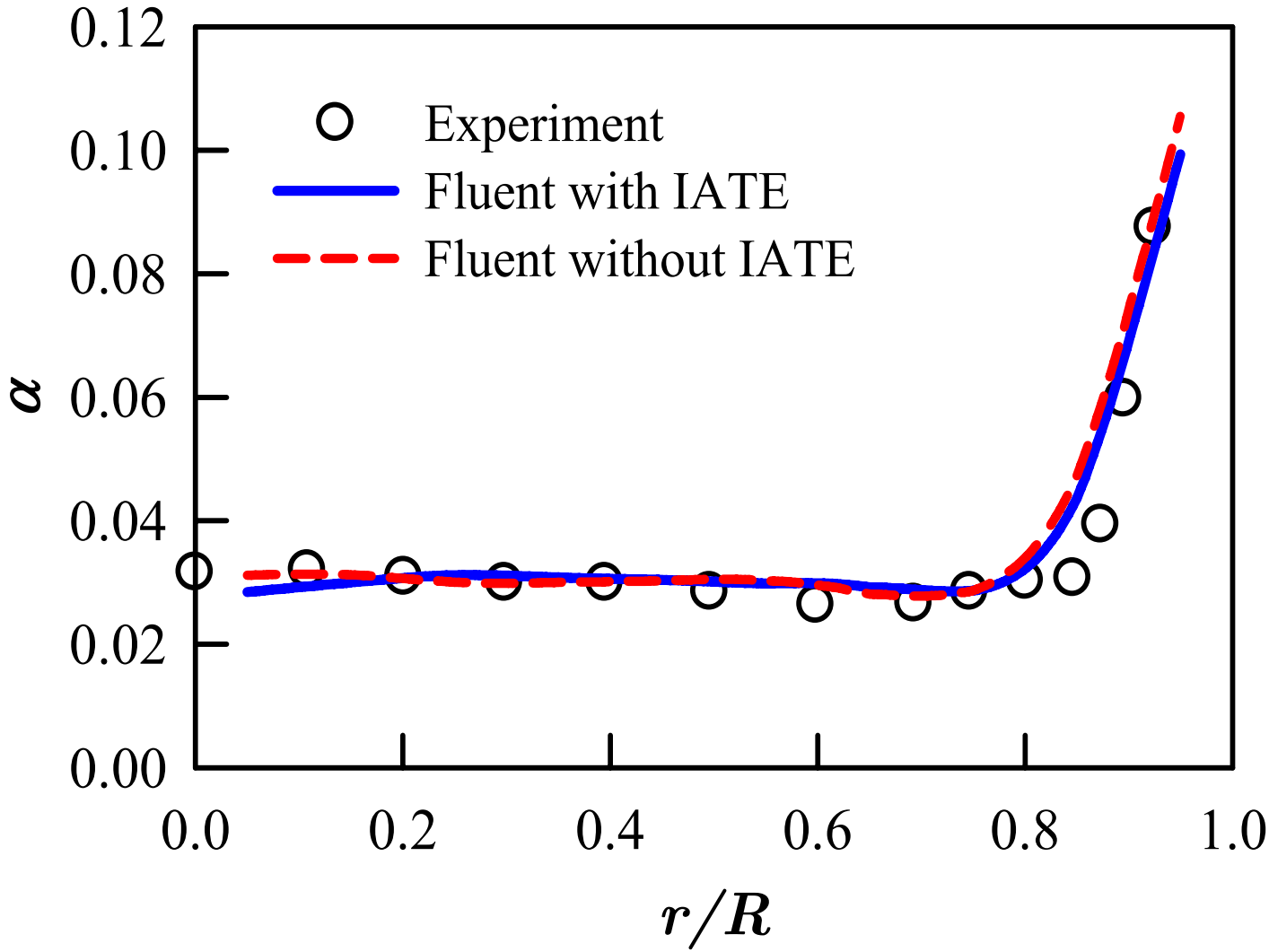

Void Fraction

Comparison: Run C-3 IAC

$(j_f = 0.49 \text{ and } j_g = 0.03 \text{ m/s})$

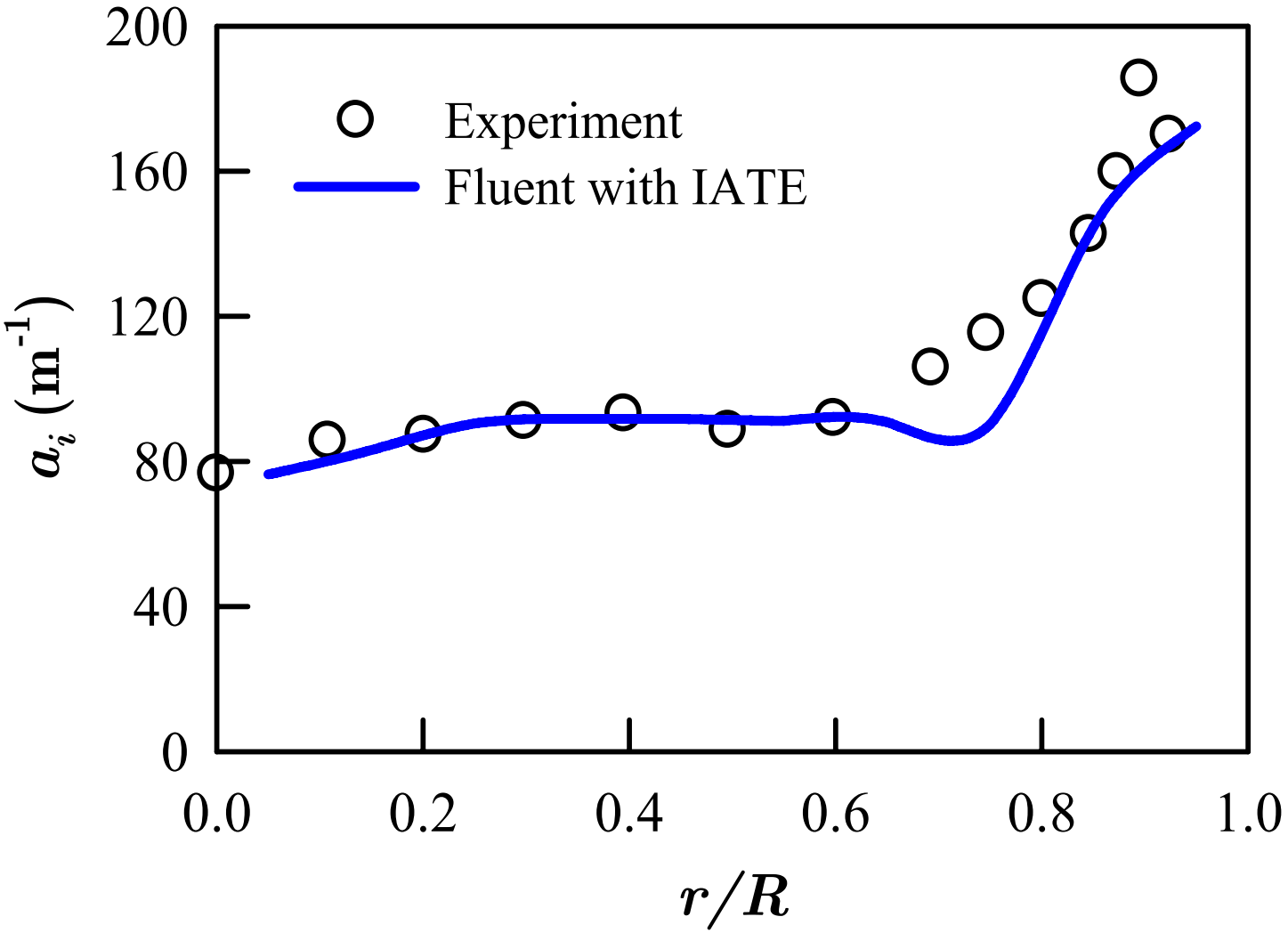

Interfacial Area Concentration

Comparison: Run C-3 D_{sm}

$(j_f = 0.49 \text{ and } j_g = 0.03 \text{ m/s})$

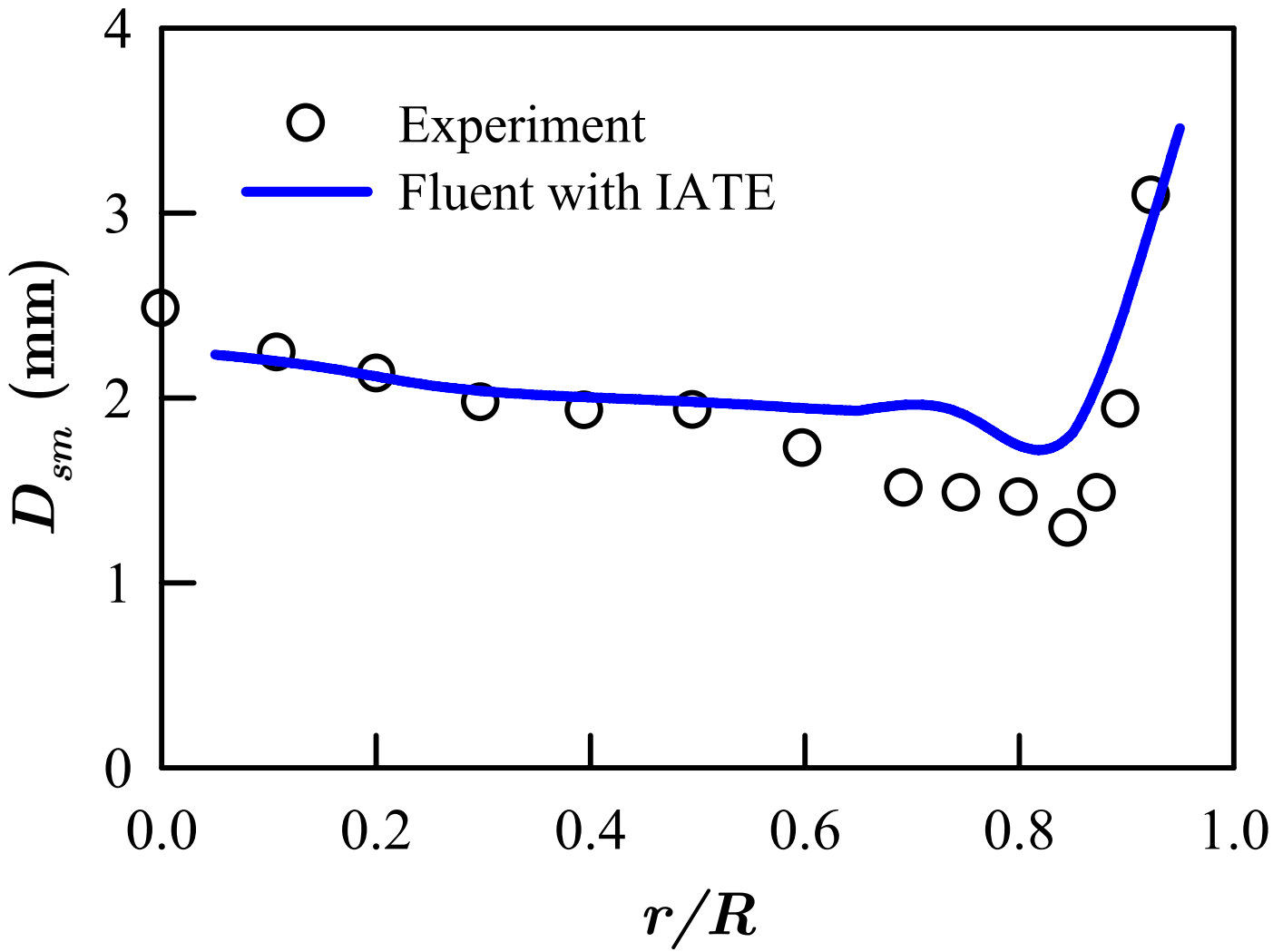

Bubble Sauter Mean Diameter

Comparison: Run C-4 VF

$(j_f = 0.99 \text{ and } j_g = 0.32 \text{ m/s})$

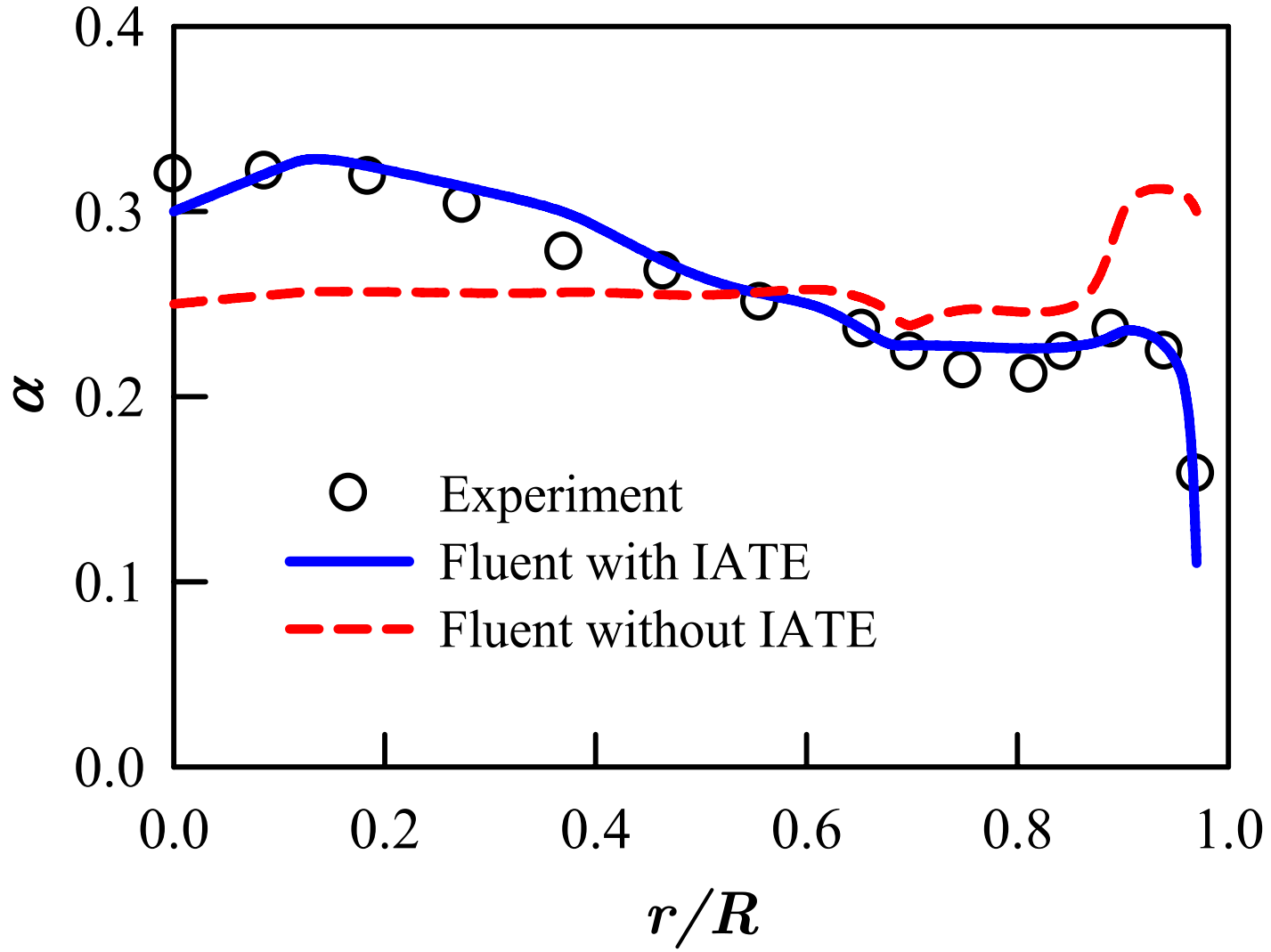

Void Fraction

Comparison: Run C-4 IAC

$(j_f = 0.99 \text{ and } j_g = 0.32 \text{ m/s})$

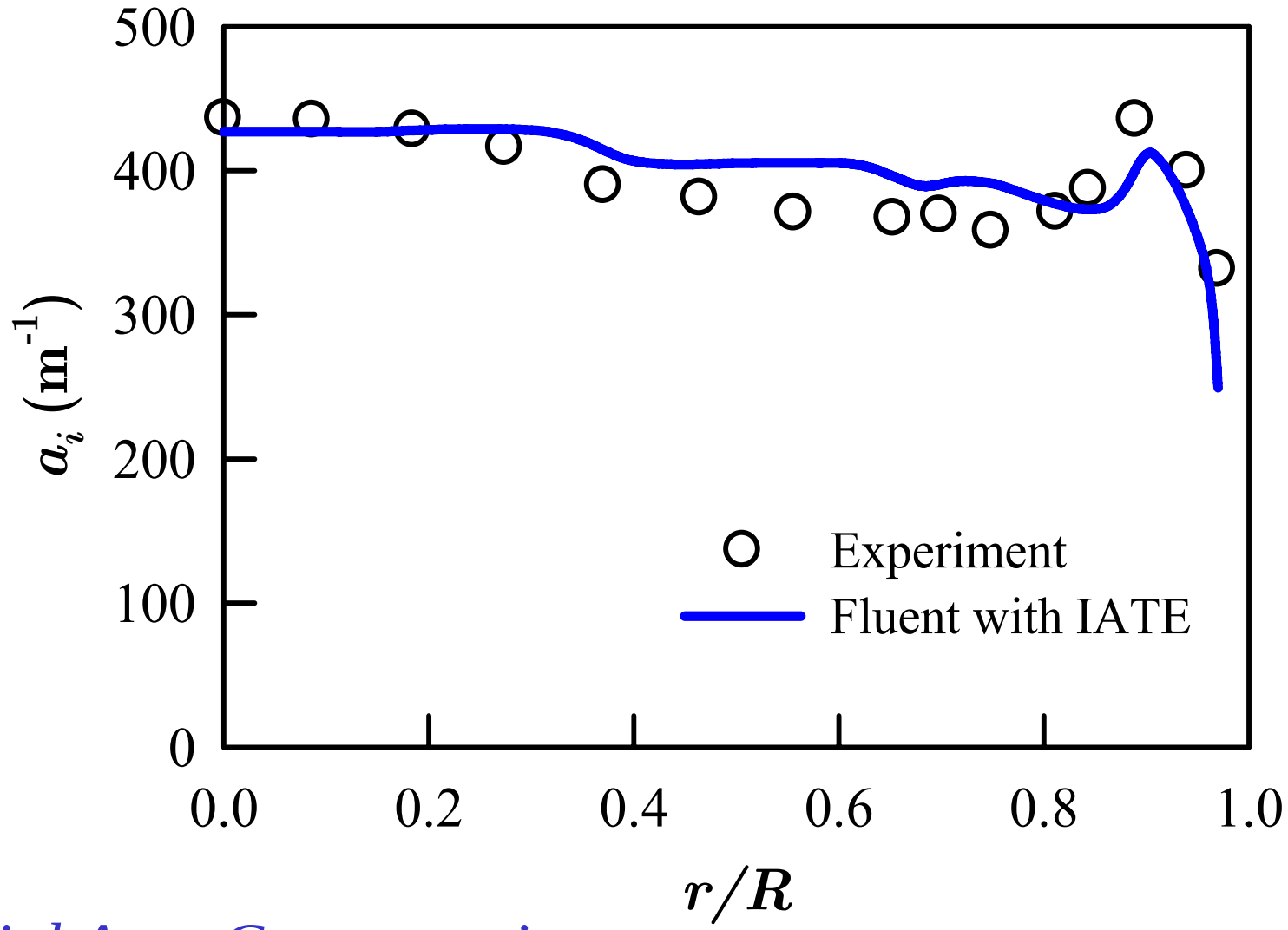

Interfacial Area Concentration

Comparison: Run C-4 D_{sm}

$(j_f = 0.99 \text{ and } j_g = 0.32 \text{ m/s})$

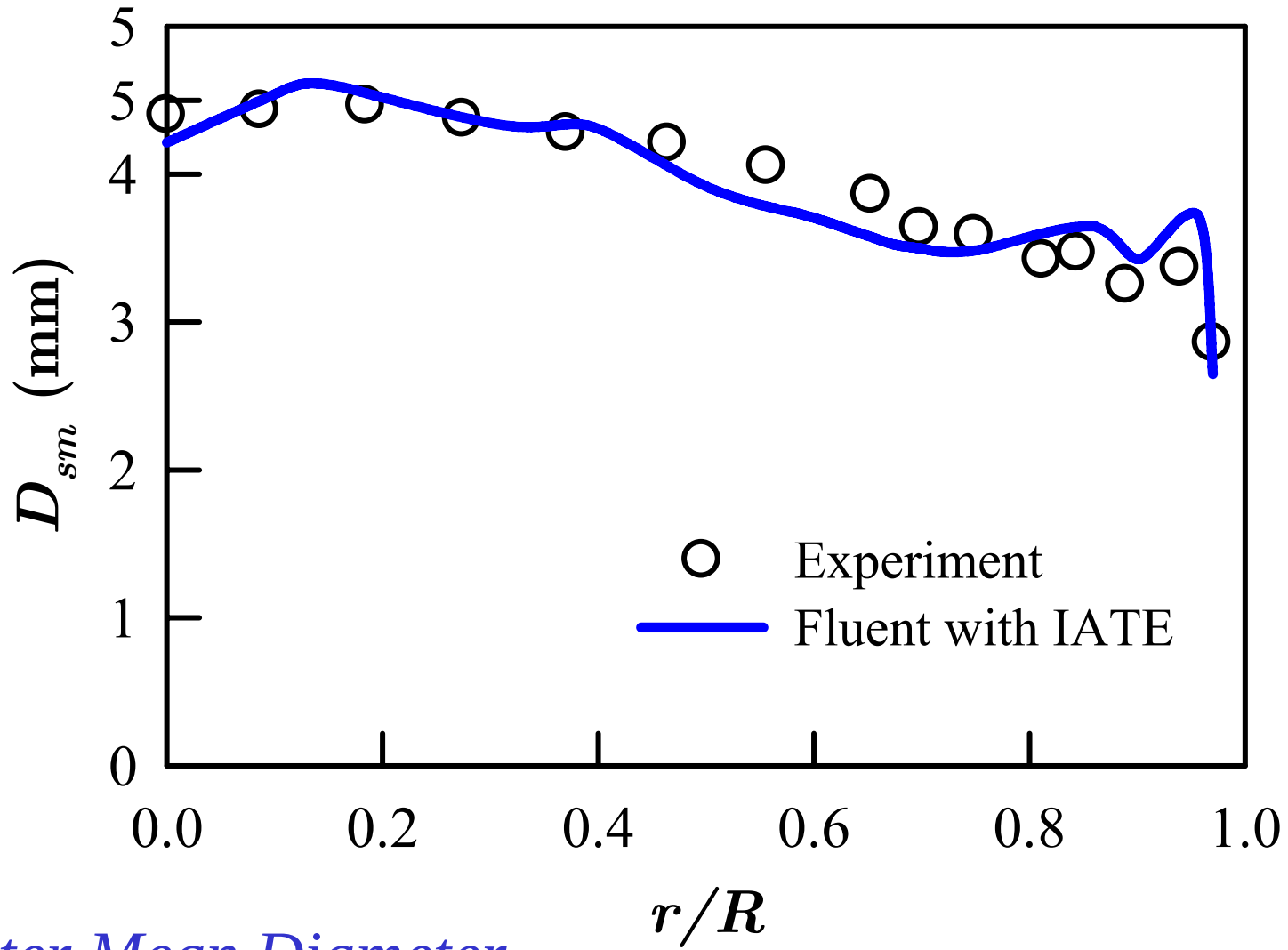

Bubble Sauter Mean Diameter

Summary and Conclusions

- The interfacial area transport equations applicable to bubbly, cap-bubbly, and churn-turbulent flows have been developed through theoretical modeling of bubble interaction mechanisms.

- 1-D steady-state one-group and two-group interfacial area transport equations have been evaluated based on the experimental data obtained from intermediate to relatively-large pipe sizes and confined rectangular flow channel.

- Overall agreement of total interfacial area concentration between the experimental data and model predictions is satisfactory, within ±10% difference.

Summary and Conclusions (Cont'd)

- The FLUENT-IATE 2-D calculations provide better agreement with the experimental data than those without the IATE in phase radial distribution.

- The preliminary results indicate that the FLUENT-IATE approach could help improve the code performance for gas-liquid two-phase flows.